AD-A132 726 MOLECULAR JET STUDY OF ANILINE-HELIUM VAN DER WAALS MOLECULES AND ANILINE.. (U) COLORADO STATE UNIV FORT COLLINS DEPT OF CHEMISTRY E R BERNSTEIN ET AL. 1/1

UNCLASSIFIED 16 SEP 83 TR-11 N00014-79-C-0647 F/G 7/3 NL

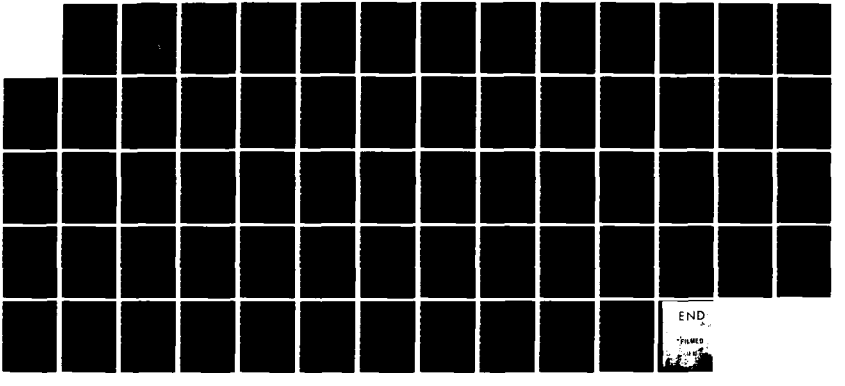

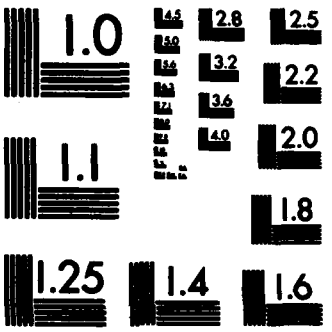

OFFICE OF NAVAL RESEARCH
Contract N00014-79-C-0647

TECHNICAL REPORT #11

MOLECULAR JET STUDY OF ANILINE-HELIUM van der WAALS MOLECULES AND ANILINE RADIATIONLESS RELAXATION IN THE $^1B_2$ EXCITED ELECTRONIC STATE

by

E.R. Bernstein, K. Law and Mark Schauer

Prepared for Publication
in the
Journal of Chemical Physics

Department of Chemistry
Colorado State University
Fort Collins, Colorado 8052

September 16, 1983

Unclassified

SECURITY CLASSIFICATION OF THIS PAGE (When Data Entered)

REPORT DOCUMENTATION PAGE		READ INSTRUCTIONS BEFORE COMPLETING FORM
1. REPORT NUMBER Technical Report #11	2. GOVT ACCESSION NO. A132726	3. RECIPIENT'S CATALOG NUMBER
4. TITLE (and Subtitle) Molecular Jet Study of Aniline-Helium van der Waals Molecules and Aniline Radiationless Relaxation in the $^1B_2$ Excited Electronic State		5. TYPE OF REPORT & PERIOD COVERED Technical Report 6. PERFORMING ORG. REPORT NUMBER
7. AUTHOR(s) E.R. Bernstein, K. Law, Mark Schauer		8. CONTRACT OR GRANT NUMBER(s) N00014-79-C-0647
9. PERFORMING ORGANIZATION NAME AND ADDRESS Colorado State University Department of Chemistry Fort Collins, Colorado 80523		10. PROGRAM ELEMENT, PROJECT, TASK AREA & WORK UNIT NUMBERS
11. CONTROLLING OFFICE NAME AND ADDRESS Office of Naval Research Arlington, Virginia 22217		12. REPORT DATE September 16, 1983 13. NUMBER OF PAGES 64
14. MONITORING AGENCY NAME & ADDRESS(if different from Controlling Office)		15. SECURITY CLASS. (of this report) Unclassified 15a. DECLASSIFICATION/DOWNGRADING SCHEDULE

16. DISTRIBUTION STATEMENT (of this Report)

This document has been approved for public release and sale; its distribution is unlimited.

17. DISTRIBUTION STATEMENT (of the abstract entered in Block 20, if different from Report)

18. SUPPLEMENTARY NOTES

19. KEY WORDS (Continue on reverse side if necessary and identify by block number)

fluorescence excitation, dispersed emission, time of flight mass spectroscopy, vibrational predissociation, molecular jet

20. ABSTRACT (Continue on reverse side if necessary and identify by block number)

Fluorescence excitation (FE), dispersed emission (DE), and time of flight mass spectroscopy (TOFMS) techniques are employed to study the van der Waals molecules formed in a molecular supersonic jet of aniline and helium ($AnHe_x$). It is found that $AnHe_1$, $AnHe_2$, and $AnHe_3$ have absorption bands that fall under all the $An(v')$ vibronic features in the $^1B_2$ electronic state of An. The features to the high energy side of the An vibronic transitions are tentatively associated with vibrations of the above van der Waals

DD FORM 1 JAN 73 1473 EDITION OF 1 NOV 65 IS OBSOLETE

Unclassified

SECURITY CLASSIFICATION OF THIS PAGE (When Data Entered)

molecules. The DE from both An and $AnHe_x$ can be characterized as either "relaxed" or "unrelaxed" depending on whether or not the aniline vibronic state emitting is the same as or different from that which was pumped. All "relaxed" An emission can be associated with vibrational predissociation of the $AnHe_x$ species. All "unrelaxed" emission from $AnHe_x$ ($\nu'+v$), with ν' = An mode and v = vdW bond mode, can be associated with $\Delta v = 0$ transitions from $AnHe_x$. A number of other relaxation mechanisms are presented and discussed including collisional ones. Some time estimates for the major processes can be discussed.

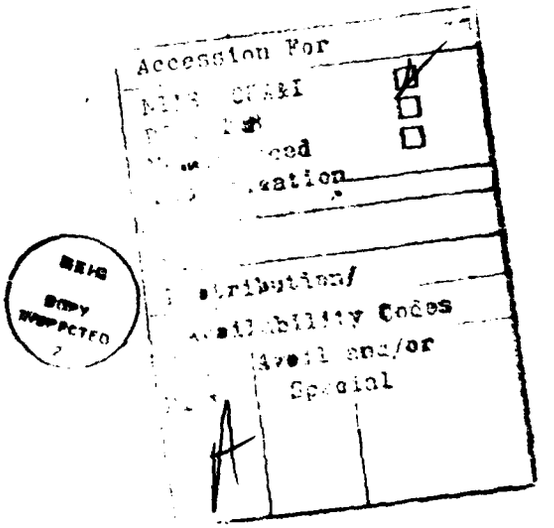

I. INTRODUCTION

The process of solvation and, more generally, the study of intermolecular interactions and potentials in the liquid state, have long been of considerable interest.[1] Recently, small clusters of molecules produced in a supersonic molecular jet have been employed to study and model condensed phase static and dynamic behavior.[2] Our motivation in constructing a molecular jet apparatus and investigating clusters is to compare the interactions and dynamics found in these microscopic van der Waals clusters with the bulk data obtained from real liquid solutions. By comparing spectroscopic and kinetic information on these clusters with similar data from cryogenic solutions[3], it is hoped that detailed information can be obtained concerning solvent-solute interactions and dynamics in real liquids.

As a first experiment on this apparatus, aniline seeded into a He carrier gas (An He) was chosen. This system has been extensively explored previously in a molecular jet[4-7], as well as in the static gas.[8,9] More recently aniline has been employed as a probe for intramolecular energy redistribution in static gases at room temperature[9] and in a cold molecular beam.[5,6]

In addition, relaxation in a variety of systems has been explored both in collisional[10] and collisionless regimes.[11] The role played by van der Waals complexes in relaxation processes has also been considered. Relaxation can be operationally defined, for our purposes, as the process by which a vibronically excited species changes its vibronic state before fluorescing. It is well known that these species vibrationally predissociate to form uncomplexed species in a lower vibronic state.[12] van der Waals complexes have also been considered as possible intermediates in collisional relaxation

of monomer species.[13] It has also been suggested that low energy collision scattering resonances or the formation of "weak van der Waals ccmplexes" can relax "monomers" in a molecular jet system over very long distances.[5,6,10,14]

Reported in this paper are the results of three experiments on An He expanded in a supersonic molecular jet: fluorescence excitation (FE) of the $^1B_2$ excited state observed for An and An He_x; dispersed emission (DE) obtained while pumping various $^1B_2$ vibronic features of An and An He_x; and time of flight mass spectroscopy (TOFMS) obtained by resonance enhanced two photon (one color) photoionization of An and An He_x. There are three major objectives of this work that are presented in the present report: a) identification and characterization of $AnHe_x$ van der Waals molecules; b) determination of bond and vibrational energies for these systems; and c) elucidation of the excited state dynamics and relaxation mechanisms which control the spectroscopic line width, emission properties, and vibrational predissociation of van der Waals species.

Through these experiments, several important aspects of the radiationless relaxation processes for An and An He_x have been explored. Although the results of FE and DE experiments do not significantly differ from those previously published[4,5,7], a number of interpretational differences are presented. New data from TOFMS experiments indicate that all of the relaxation associated with An monomers can actually be attributed to vibrational predissociation of $AnHe_x$ at large distances from the nozzle. These studies emphasize that the three spectroscopic techniques FE, DE, TOFMS are complementary and are often essential for the complete study of relaxation and complexation in a molecular jet. Geometry and bond strength for An He_x van der Waals complexes will be addressed in subsequent publications.

II. EXPERIMENTAL

The supersonic molecular jet apparatus used in these experiments is a two chamber system as shown in Fig. 1. The carrier gas (commercial grade He) is regulated to the desired nozzle backing pressure (P_o) and is passed through a trap containing the solute (reagent grade An). The trap containing An is kept at room temperature and the concentration of An in the beam varies as P_o is changed.

This mixture is delivered to either a continuous (CW) nozzle or a pulsed nozzle. The CW nozzle consists of a commerical pinhole (25 μm in diameter) clamped between two stainless steel plates. The plate on the low pressure side of the pinhole is machined such that its orifice is at the apex of a 120° cone. This minimizes the interaction of the plate with the cold beam. The pulsed nozzle is manufactured by Quanta Ray and is of the Gentry design operated at 10 Hz with an open time of ~100 μs. Its orifice is 0.5 mm in diameter and the maximum backing pressure for this valve is ~220 psi.

The first chamber is evacuated by an Edwards oil vapor booster pump backed by an Edwards 150 cfm dual stage mechanical pump. With this pumping system it is possible to maintain a chamber pressure (P_1) of $\leq 1 \times 10^{-3}$ torr with P_o = 1000 psi backing the CW nozzle. With $P_o \geq 1000$ psi , the oil vapor booster pump begins to saturate and further increase in P_o results in dramatic fluctuations in P_1 until P_1 is determined by the pumping speed of the mechanical pump.

Both FE and DE experiments are done in the first chamber. For the FE experiment, a tunable Nd/YAG pumped dye laser output is doubled and focused by a 1 m lens into the chamber perpendicular to the molecular beam axis. The

optical path is baffled both entering and exiting the chamber to reduce scattered light in the detection system. Emission from the intersection of the molecular beam and the laser beam (0.5 cm downstream from the nozzle, X_{CW} = (downstream distance/nozzle diameter) -200) is collected by a lens system the axis of which is perpendicular to the two above mentioned beams. The image of the intersection region is focused onto the cathode of a cooled photomultiplier tube (RCA C31034-A02) mounted on a translation stage below the chamber.

For the DE experiment the emission is directed by a prism onto the slits of a 1 m monochromator (McPherson 2051) with a 1200 groove/mm grating (used in 3rd order). Reported intensities are not corrected for the grating response curve. Detection is also by a cooled C31034-A02 photomultiplier tube. The signal from the photo tube is processed in both experiments by a PAR 162/164 boxcar averager and output to a chart recorder or a computer.

For the TOFMS experiments the molecular beam is skimmed (Beam Dynamics, 1 mm skimmer) between the two chambers and brought into the second chamber. The second chamber is maintained below 5×10^{-7} torr (P_2) at maximum gas loads by a 10" Varian diffusion pump. The ionization region of the TOFMS (Quanta Ray) is centered in second chamber and a single Nd/YAG pumped doubled dye laser beam is focused into the chamber perpendicular to the molecular beam axis without baffling. The ions are accelerated by a 5000V potential into a flight tube perpendicular to both the laser and molecular beams. The ions are detected by a Galileo microchannel plate. The flight tube and ionization region are cooled by a liquid nitrogen trap; the tube is independently pumped by a 6" diffusion pump. Signals from the multichannel

plate detector are analyzed on a transient digitizer (Tektronix 7912AD) and averaged and processed on an HP9845S computer.

The signal from the two photon ionization of An and An He_x clusters is greatly enhanced if the photon is resonant with a vibronic level of the $^1B_2$ state of An. Therefore, the signal from one mass channel of the TOFMS as a function of laser wavelength is an absorption spectrum of the mass species being monitored. Ions created in the above manner have 7000 cm^{-1} excess vibrational energy. The $AnHe_x$ clusters that are ionized tend to dissociate to smaller clusters or the monomer. In future experiments a two color photoionization will be employed such that the excess ion vibrational energy will be close to zero.[15]

Error in the tabulated frequencies for the FE experiments is determined by the reproducibility of the dye laser wave length dial (± 2 cm^{-1}). The dye laser monochromater combination has a systematic error of less than 2 cm^{-1}. Random measurement error in the DE experiment is less than 1 cm^{-1} for sharp lines. Linewidths for the DE experiments are slitwidth limited at ~8 cm^{-1}.

III. RESULTS

FE spectra of An expanded with He at various backing pressures P_o show the existence of absorption due to An He_x van der Waals clusters. Fig. 2 shows FE spectra of the 0_0^0 region of An at different P_o. At low backing pressures ($P_o \leq 200$ psi) absorption due to An monomers only is observed. As the backing pressure is increased, peaks due to the 0_0^0 absorption bands of different An He_x clusters are seen at higher energy. Some of these features may also be associated with vibrations of the van der Waals complexes built on these origins.[16] The peaks are listed in Table I. Notice that at high backing pressures the monomer peak becomes broad and asymmetric to the high energy side. This suggests that peaks due to An He_x may be hidden beneath the monomer feature, unresolved in this experiment. Mass spectra that support this supposition will be discussed below.

The generalization used by others[12b] that consecutive addition of He atoms to a monomer gives rise to additive spectral shifts breaks down in this system. Different geometries due to binding of He atoms to inequivalent sites may produce different spectral shifts for the same size $AnHe_x$ cluster. Also, as pointed out above, some of these peaks could be due to or distorted by van der Waals bond vibrations. Previously, pressure studies have been used to differentiate between features due to clusters of different sizes.[16a] Fig. 3 shows a graph of the pressure dependence of some of the $AnHe_x$ peaks associated with the An monomer 0_0^0 feature. At pressures for which the individual peaks are well defined, the pressure dependence has already begun to fall off and the limiting value of the pressure vs. intensity slopes as $P_o \rightarrow 0$ cannot be readily determined. Similar observations are valid for other An

vibronic transitions. Fig. 4 and Table II show the data for the absorption peaks near the An $10b_0^2$, $6a_0^1$, I_0^2 and 1_0^1 transitions. The vibration notation for An can be found in refs. 4, 5, 6, 8, 9 and is quite standard. It parallels that used for benzene except that I denotes the NH_2 inversion mode.

TOFMS data are useful in further understanding the above absorption and emission data. Fig. 5 presents the mass spectrum obtained while pumping the monomer 0_0^0 feature as a function of P_o. At low pressure, only monomer An is seen with associated C^{13} peaks. As P_o is increased, mass peaks associated with AnHe, $AnHe_2$, and $AnHe_3$ are clearly discerned. This observation indicates the existence of absorption features associated with $AnHe_x$ hidden under the main monomer 0_0^0 peak. As the monomer peak is pumped, part of the 0_0^0 absorption lines of AnHe, $AnHe_2$, and $AnHe_3$ are also pumped. Power broadening is eliminated as a cause of the extra mass peaks because the laser power has been kept low (~0.5 mj/pulse) and constant throughout this series of experiments, and is quite comparable to that reported for similar studies.

Fig. 6 presents the mass spectra observed by pumping various $AnHe_x$ features of 0_0^0 region spectrum. A good deal of cluster fragmentation is evident in these results; even as peak 6 is pumped, the strongest feature in the mass spectrum is the An monomer.

On the other hand, the mass spectrum arising from pumping the region 350 cm^{-1} higher in energy than the 0_0^0 transition ($10b_0^2$ and $16a_0^2$) evidences intensity only in the monomer channel even at high backing pressure (P_o = 900 psi). Fig. 7 gives a trace of the mass spectra taken while pumping

the $10b_0^2$ monomer peak, the $16a_0^2$ monomer peak, and a van der Waals peak. The fact that no $AnHe_x$ mass features are seen indicates that the vibrational energy in the An molecule pumped to the $10b^2$ state is enough to vibrationally predissociate the $AnHe_x$ complexes.

DE spectra of An monomers in a molecular jet have previously been reported.[4,5] Careful analysis of all data available has led us to interpretations of these data that differ from those previously published. The implications these spectra have for the understanding of collisional relaxation of An monomers in the beam will be discussed in detail in the next section. In presenting the results of the DE experiments, groups of emission peaks that originate from a particular vibronic level other than the one originally pumped will be referred to as relaxed emission. This terminology can be somewhat misleading, however, because our evidence suggests that such fluorescence does not originate from the relaxed pumped An monomer but originates instead from dissociated $AnHe_x$ clusters under the beam conditions set forth in the last section.

0^0: Fig. 8 and Table III present the emission spectra obtained by pumping the 0_0^0 monomer and a van der Waals absorption band. Direct fluorescence from the 0^0 vibronic level to several totally symmetric vibrations in the ground state constitute a pattern that will be referred to as a family. A comparable "family" of peaks results from the direct fluorescence of any vibronic level and the presence or absence of members of a family can, in general, aid in assigning emission peaks to an emitting level. For the DE spectra, members of a family are marked together and labeled according to the first feature in the family. The DE spectrum of the van der Waals peaks in the 0_0^0 region is identical to the monomer 0_0^0 DE spectrum. While there are a

number of mechanisms which might be postulated to reproduce this observation, the most likely explanation is that the cluster feature being pumped is a van der Waals vibration built on the cluster 0_0^0 transition. The cluster 0_0^0 peak itself is buried under the monomer 0_0^0 peak. The transition observed does not involve a change in van der Waals bond vibration and thus would be isoenergetic with the monomer 0_0^0 emission. All of the possible fluorescence pathways for $AnHe_x$ will be discussed further in the next section.

$10b^2$, $16a^2$: The absorption spectrum of An shows a doublet feature at about 352 cm^{-1} above the 0_0^0 (see Fig. 4). This feature has previously been assigned as the I_0^1 transition.[7] However, Fig. 9 and Table IV show that the emission spectra from these two levels differ from one another and from the known emission spectrum of I^1 observed by I_1^1 pumping. We were able to reproduce a weak I^1 emission spectrum even though the I_1^1 absorption feature is quite weak in the molecular jet. Consequently, these two absorption features have been reassigned to be consistent with the apparent relaxation seen in their emission spectra.

Fig. 10 and Table V present the emission spectra of the $10b^2$ monomer and a van der Waals peak at high P_o. The monomer peak emission evidences substantial apparent relaxation to three different levels, the $10b^1$, 0^0, and $16a^2$. The van der Waals feature pumped exhibits an emission spectrum consisting entirely of peaks that can be identified with the relaxed monomer emission peaks that one would expect from the $16a^2$ and the $10b^2$ levels.[9]

$6a_0^1$: Fig. 11 and Table VI present the emission data for the $6a_0^1$ monomer and van der Waals absorption features. The apparently relaxed emission peaks increase dramatically in intensity with increased backing pressure. The

spectra obtained by pumping van der Waals absorption features show increased relaxation along the pathways evidenced in the monomer spectrum as well as peaks that correspond to unrelaxed $6a^1$ monomer emission.

I_0^2: Fig. 12 and Table VII present the emission data obtained by pumping the I_0^2 monomer absorption feature. Although the spectrum looks qualitatively similar to spectra previously published[5], some assignments are different. Because of the extensive overlap in the lower energy congested region of the spectrum, the assignments rely heavily on the consistency of various peaks with expected positions and intensities of other family members. For example, the only direct evidence for emission from the $I^1 16a^1$ is the small peak at 729 cm^{-1} below the pump line, but the other members of the family should be buried under intense members of the I_2^2 family. This assignment is consistent with the apparent enhancement of the peaks at 1522 and 1706 cm^{-1} below the pump line.

1_0^1: Fig. 13 and Table VIII describe the emission spectrum as the 1_0^1 monomer feature is pumped. This spectrum is extremely congested at longer wave lengths and nearly all the apparent relaxation peaks are coincident with possible unrelaxed features. Many of the peaks are shown to have a relaxed component from variation of P_o; others are identified as having a relaxed component because their intensity is greater than would be expected for a normal unrelaxed family member. The assignment of apparently relaxed families explains the intensity anomalies in the spectrum.

Results using a pulsed nozzle are consistent with those reported above using a CW nozzle. At P_o = 200 psi, the beam density at the downstream observation point for the pulsed nozzle [$X_{pulsed} \approx 10$] is comparable to the

CW nozzle at P_o = 400 psi but the value of P_1 is much smaller for the pulsed nozzle. [It should be noted that in the work of ref. 5 and 6, X_{pulsed} is typically below 5.] The amount of apparent relaxation in the pulsed nozzle system at P_o = 200 psi is comparable to the CW system at P_o = 400 psi for the $10b_0^2$ emission spectrum (X_{CW} ~ 200). Therefore, beam relaxation in our system is not due to background gas nor is it dependent upon the point of observation in the beam.

IV. DISCUSSION

In this section, discussion will focus on the TOFMS data and its central role in the understanding of the FE and DE experiments. One of the most important contributions that the mass spectral studies make is to help in the assignment of features in the FE and DE spectra to specific mass species. In the 0_0^0 region, Fig. 5 conclusively demonstrates that the monomer absorption peak has hidden within its width components due to several mass species. Fig. 6 indicates that peak 2 in this region is largely due to $AnHe_2$, while peak 3 is largely due to the AnHe species. Although these data are complicated by fragmentation, other data support these assignments as well. Preliminary frequency scans, using the TOFMS gated on the different mass channels as a detector, support the above observations. These experiments yield slightly red shifted 0_0^0 peaks for the AnHe and $AnHe_2$ species and several peaks to the blue of the monomer 0_0^0 due to vibrations of the van der Waals bond. Further two color ionization and other studies are underway in order to quantify the shifts and confirm these assignments.

The TOFMS data also contribute significantly to the understanding of the DE experiments. Because the mass spectral data have shown clearly the existence of van der Waals absorption features hidden under the monomer 0_0^0 absorption band (and, therefore, presumably under higher monomer vibronic features as well), several mechanisms that could result in apparently relaxed emission now become possible. Under these circumstances, both monomer and van der Waals clusters are excited by a single laser frequency; dissociation of a van der Waals molecule could result in DE from levels lower in energy than the level pumped, giving rise to apparently relaxed monomer emission. Furthermore, as Fig. 7

demonstrates, pumping van der Waals features near $10b^2$ does not evidence cluster peaks in the TOFMS contrary to a similar experiment for the 0_0^0 region. This evidence leads to the conclusion that vibrational predissociation dominates the van der Waals molecule dynamics for vibrationally excited aniline. Similar observations are made as peaks in the $6a^1$ region are pumped and it is presumed that vibrational predissociation of van der Waals species is responsible for the relaxation seen in these spectra and others.[5,6]

The TOFMS data also help to resolve questions regarding some of the apparently unrelaxed emission. As shown in Figs. 8 and 11, pumping van der Waals features can generate peaks identical with unrelaxed monomer emission. It is not at all obvious how, under the conditions of these experiments, an excited van der Waals species could fragment leaving a monomer in the same excited (non-0_0^0) vibronic state. However, the observation of van der Waals absorption features within the monomer feature leaves open the possibility that the observed "unrelaxed monomer" emission arising from a pumped van der Waals feature is due to van der Waals species. The TOFMS experiments aid in the identification of the initial species created, but without knowing the species that fluoresces, it is not possible to determine the exact mechanism responsible for the fluorescence. Further TOFMS experiments will be aimed at identifying the emitting species.

Some kinetic rate information can also be extracted from the TOFMS experiments. The clear identification of complete vibrational predissociation of $AnHe_x$ due to An vibrations of energy greater than 350 cm^{-1} allows the rate of this process to be bracketed by the absorption line width and the excited state lifetime. These results also indicate a surprisingly slow rate

for the ionization process. Changes in the ionization process may lead to better estimates of the rate of vibrational predissociation and/or better understanding of the ionization process itself.

The remainder of this section will focus largely on a detailed discussion of the DE data, and will be organized into four parts. First, a complete enumeration of the possible mechanisms which can be responsible for the DE spectra will be presented. Second, the mechanisms which can lead to apparently relaxed emission will be discussed. Third, the unrelaxed emission will be treated. Finally, the kinetic information which can be gathered from these experiments will be presented in more detail.

A. Mechanisms

The TOFMS experiments are of fundamental importance to this study as they can be employed to identify the species initially prepared and observed in the PE spectra. Therefore, the tabulated mechanisms below are grouped according to the initially prepared species. In some cases, the processes which take one species to another are not well understood or cannot easily be differentiated. Moreover, it is possible that more than one mechanism contributes to the overall observed spectrum. However, an effort has been made to identify all possible contributions which might lead to the observed DE spectrum.

A central issue raised by the discussion of these mechanisms deals with the importance of collisions in this system. It is found that there is no <u>necessity</u> to postulate the presence of collisional resonance mechanisms for the explanation of the observed DE spectra under the beam conditions used in this work ($X > 10$); other mechanisms, apparently more plausible, can be suggested. Calculations show that hard sphere collisions between An and He

occur on the average about 1 every 50 to 100 An or $AnHe_x$ excited state lifetimes. Nonetheless, weak scattering resonance interactions have been postulated to explain data similar to those presented here,[5,6] but for $X < 10$. Therefore, all mechanisms including collisional ones, will be discussed below.

Seven possible mechanisms can be initially considered. They involve: a) single vibronic level fluorescence (SVLF) of an excited monomer species; b) collisionally induced relaxation (CIR) of an excited monomer species followed by fluorescence (F); c) vibrational predissociation (VP) of a van der Waals molecule followed by monomer F; d) collisionally induced dissociation (CID or CIDR) that may or may not change the An vibronic level intensity excited followed by F; e) SVLF of a van der Waals molecule $AnHe_x$; f) relaxation, either collisionally induced (CIR) or by intramolecular vibrational relaxation (IVR) of a van der Waals vibration followed by F of the van der Waals species; and g) VP of $AnHe_x$ by a van der Waals vibration followed by F from a smaller van der Waals molecule, e.g. AnHe or $AnHe_2$. These mechanisms can be schematically represented by the following equations:

U a) $An^*(\nu') \xrightarrow{SVLF} An$

R b) $An^*(\nu') \xrightarrow{CIR} An^*(\nu'-n) \xrightarrow{F} An$

R c) $AnHe_x^*(\nu') \xrightarrow{VP} An^*(\nu'-n) \xrightarrow{F} An$

U or R d) $AnHe_x^*(\nu') \xrightarrow[CIDR]{CID} An^*(\gamma') \xrightarrow{F} An$

U e) $AnHe_x^*(\nu'+v) \xrightarrow{SVLF} AnHe_x(v)$

U f) $AnHe_x^*(\nu'+v) \xrightarrow[IVR]{CIR} AnHe_x^*(\nu') \xrightarrow{F} AnHe_x$

U g) $AnHe_x^*(\nu'+v) \xrightarrow{VPvdW} AnHe_{x-1}^*(\nu') \xrightarrow{F} AnHe_{x-1}$

in which U and R label processes responsible for unrelaxed or relaxed emission,

respectively, An^* and $AnHe_x^*$ signify an excited electronic $^1B_2$ state species, ν' is some vibrational quanta for An in the excited electronic state, γ' is some vibration quanta that is equal to or lower in energy than ν', $\nu'-n$ ($n \geq 1$) is some lower An vibrational excitation in the $^1B_2$ state, and v is some quanta of a van der Waals vibrational mode.

B. Relaxed Emission

If only a specific vibronic state of the monomer is populated, relaxed emission can only result from collision induced relaxation (process b). This mechanism has been proposed to explain observations of DF in a region of a supersonic molecular beam with a higher collision rate than the one reported in this work.[5,6] However, the relaxed emission seen in the higher collision rate experiment is nearly identical with that observed in the present experiment. Based on these observations, there must be some doubt that collisions are important for either experiment.

It has been pointed out previously that the TOFMS data clearly show the existence of van der Waals absorption features hidden under the monomer absorption peaks. If the laser frequency is tuned to a monomer absorption, the same vibronic level of probably at least two van der Waals species will also be excited. The behavior of an excited van der Waals species can be explored independently by tuning to a van der Waals absorption feature away from the monomer feature. Several figures (notably 10 and 11, but others as well) show that relaxation dominates the spectrum of van der Waals molecules.

Mass spectra of several peaks in the $10b^2$ and 6_a^1 regions show that vibration predissociation of the van der Waals molecules does occur in these systems. None of the peaks in these regions shows recordable intensity in the

van der Waals mass channels. Therefore, VP must be complete before ionization can occur. Also, recombination of An^+ with He is not contributing to intensity in the van der Waals channels in the 0_0^0 mass spectrum, as this process would be equally likely for the mass spectra in the $10b^2$ and 6_a^1 region. Although only the 0_0^0, $10b^2$ and 6_a^1 region mass spectra have been studied in detail so far, it appears the VP is occurring for all the vibronic levels except 0_0^0, and can be invoked to explain all of the observed relaxation in the An/He system.

Process d could also lead to relaxation if the dissociation of the van der Waals species is accompanied by loss of vibration energy in the excited An. However, as pointed out previously, calculations show that such energetic collisions do not readily occur under the present conditions. Mass spectral data further suggest that collision induced dissociation and relaxation is certainly less important than VP of van der Waals molecules because collision induced dissociation should be equally probable for species in the $10b^2$ or 0^0 state where as VP cannot occur for species in the 0^0 state. The fact that $AnHe_x$ features are observed in the 0_0^0 band for the TOFMS and not in the 6_a^1 or $10b^2$ TOFMS clearly indicates that VP dominates for the vibronic excited states of $AnHe_x$ as the mechanisms for generation of relaxed emission from An monomers.

Further evidence against process (b) under the conditions of these experiments can be found in an experiment with An and CH_4 seeded into the He carrier gas.[18] With CH_4 at low concentration ($\leq$0.5%) in the expansion gas, considerably less relaxation is observed in the DE experiments from the $6a^1$ pumped level and less intensity is observed for the $AnHe_x$ FE spectra. Thus, CH_4 competes with He to form van der Waals clusters with An. The An intensity

is roughly the same in both experiments. $An(CH_4)_x$ clusters do not have absorption bands which overlap with the An monomer peaks as can be demonstrated by TOFMS spectra. Therefore, process (b) is not very important and the other processes are largely responsible for the relaxed emission from vibronic "monomer" and $AnHe_x$ features.

C. Unrelaxed Emission

At low backing pressure there is no question that An(ν') SVLF (a) dominates the system; at low P_o ($\leq$200 psi) few van der Waals molecules are produced. However, at higher backing pressure van der Waals species can produce emission identical (within our stated resolution) with that of An monomers prepared in the same aniline vibronic state. The van der Waals peaks near the 0^0 produce apparently unrelaxed emission exclusively because these species cannot undergo VP. As shown in Fig. 11, van der Waals peaks near 6^1_a show some unrelaxed emission features, although most of the emission is relaxed emission. van der Waals peaks near $10b^2$ do not show unrelaxed emission presumably because VP is so facile from this An vibronic state. van der Waals species in other vibronic states should show varying amounts of unrelaxed emission depending on the rate of VP for the particular An vibronic level.

The TOFMS data presented earlier suggest two conclusions: absorption peaks for a given vibronic level of AnHe and $AnHe_2$ are under the same vibonic band for the monomer; and the resolved van der Waals peaks to the blue of the monomer involve vibrations of these two van der Waals species. This assignment is necessary if processes e,f,g are occurring and this assignment will be assumed in the subsequent discussion. If the assumption is incorrect and these blue shifted features are different van der Waals species, then the only

mechanism consistent with the results is d. The problems associated with this latter mechanism will be discussed below.

The most direct process which can lead to apparent unrelaxed monomer emission from an $AnHe_x^*(v'+v)$ is SVLF to the ground state of the $AnHe_x$ complex with $\Delta v=0$ (process e). If the van der Waals vibration is the same in the ground state as in the $^1B_2$ state, as is often the situation for other systems,[19] then process e would produce the same emission as the complex with v=0 in the $^1B_2$ and therefore the DE would be nearly the same as that found for the unrelaxed monomer. This process does not require that collisions be postulated and it is consistent with the observation that changes in van der Waals vibrational quanta of zero are most intense.[19] Moreover, the observations are consistent with the force constants being the same in both ground and excited states of $AnHe_x$. It is somewhat surprising that some red-shifted intensity is not seen in the DE spectra of the van der Waals features, but this is presumably due to insufficient resolution (~8 cm^{-1} for DE experiments).

Another possibility for generation of unrelaxed emission from cluster absorption features is the dissipation of the van der Waals species vibrational energy to produce $AnHe_{1,2}(v')$. Process f involves the dissipation of van der Waals vibrational energy through very weak collisions in the beam, or through IVR made possible by a high density of states. It has recently been suggested that IVR can occur in the tetrazine-Ar system.[19] However, it seems unlikely that there is either sufficient collisions for collision induced relaxation or sufficient density of states for IVR under the circumstances of these experiments.

It is perhaps conceivable that one quanta of a van der Waals mode could vibrationally predissociate an An-He bond (process g). However, that would imply that the An-He bond energy is roughly 10 cm^{-1}. A binding energy this low does not seem to be consistent with the stability of the species (greater than 15 μsec from TOFMS) or with estimates of the tetrazine-He binding energy of greater than 57 cm^{-1}.[17] Moreover, if the blue shifted van der Waals peaks can be interpreted as vibrations, a rough Morse potential dissociation energy calculation based on ω_e ~ 9 cm^{-1} and $\omega_e X_e$ ~ 1-2 cm^{-1} gives a D_e of 100 ± 50 cm^{-1}. It thus appears unlikely that process g is terribly important in this instance.

As pointed out previously, process d cannot be ruled out as a possible mechanism for generation of unrelaxed emission from van der Waals complexes. However, because of the low collision rate and the observation that process d is not contributing appreciably to the relaxed spectra, it seems unlikely that collisional dissociation is contributing to the unrelaxed emission spectra.

To summarize the discussion of the aniline/He DE spectrum: while it is clear that SVLF dominates aniline emission at low backing pressure, at high P_o apparent aniline relaxed emission is largely due to VP of van der Waals species. Collision induced relaxation of aniline monomers is not occurring appreciably in this system and it appears unlikely that any collision processes contribute significantly to the overall beam kinetics and dynamics at X_{cw} ~ 200 or X_{pulsed} ~ 10. The apparently unrelaxed monomer emission from van der Waals species appears to be SVLF of the $AnHe_x$ excited cluster to the ground state with $\Delta v=0$ for the van der Waals vibrations, although processes f and g cannot be conclusively ruled out at this time.

D. Excited State Kinetics

The TOFMS experiments may also be used to assist in understanding the kinetics of the relaxation processes in the excited state. As pointed out previously, $AnHe_x$ clusters excited to the $10b^2$ vibronic region vibrationally predissociate before ionization can occur. This indicates that the average time between absorption of the first photon by the complex and the absorption of the ionizing photon is somewhere between the minimum lifetime of the complex (~5 ps from FE linewidths) and the lifetime of the An excited state (~5 ns). A rough calculation of the photon flux at the ionization point indicates that the quantum efficiency for ionization must be very low ($<<10^{-3}$). Such a low quantum efficiency could be due to the high excess vibrational energy (~7000 cm^{-1}) of the ion and a poor Franck-Condon factor for the neutral ion $AnHe_x$ transition. If this is correct, a two color ionization with roughly zero vibrational excess energy could ionize $AnHe_x$ from, for example, $10b^2$ before the cluster could vibrationally predissociate. Such experiments could lead to a better estimate of the time it takes for the complex to undergo vibrational predissociation. At present this time τ is found to be within the limits $5\ ps \leq \tau \leq 5\ ns$.

V. CONCLUSIONS

The supersonic molecular jet experiment is certainly an important tool for the study of van der Waals complexes and monomer dynamics. Experiments involving FE, DE and TOFMS complement one another and generate an extensive picture of the overall excited state energies and lifetimes for many processes. The major conclusions that can be reached based on this work are as follows:

1. AnHe and $AnHe_2$ features lie under the An monomer feature for all vibronic states of aniline that have been observed (e.g. 0_0^0, $10b_0^2$, $6a_0^1$, etc.)
2. van der Waals features to the blue of the aniline vibronic transitions are tentatively assigned to AnHe and $AnHe_2$ van der Waals vibrations. Some background intensity may well be associated with high order $AnHe_x$.
3. Under these low collision conditions it does not appear to be necessary to postulate either An or $AnHe_x$ collisional processes to account for either the observed DE or TOFMS data.
4. "Relaxed An emission" can be associated with vibrational predissociation of van der Waals molecules.
5. "Unrelaxed An emission" associated with pumped van der Waals features arises most likely through transitions for which the van der Waals bond vibrational excitation does not change ($\Delta v=0$). Under this mechanism all features to the blue of an aniline vibronic feature are assigned as $AnHe_x$ cluster vibrations built on the $AnHe_x^*(\nu)$ vibronic origin lying under the $An^*(\nu)$ vibronic feature.
6. The time range for VP, second photon absorption for the photoionization process, and other processes that may occur with reduced probability seems to be between ~5 ps and ~5 ns.

Further work is underway at present to use less energetic ionization to reduce fragmentation and improve the probability for absorption of the second photon. In addition, high resolution spectra will be obtained shortly to resolve rotational features of the $AnHe_x$ van der Waals molecules.

ACKNOWLEDGEMENTS

We wish to thank Professors D.H. Levy and R.E. Smalley for many helpful discussions concerning the construction and design of the apparatus and of these experiments. We also wish to thank Professor S.A. Rice for preprints of his results prior to their publication and some helpful discussion of the details of his work.

REFERENCES

1. a) O. Sinanoglu, Chem. Phys. Lett. 81, 188 (1981).

   b) J. Sunner, K. Nishizawa and P. Kebarle, J. Phys. Chem. 85, 1814 (1981).

2. a) P.M. Felker and A.H. Zewail, Chem. Phys. Lett. 94, 454 (1983).

   b) A. Amirav, U. Even and J. Jortner, J. Chem. Phys. 75, 2489 (1981).

   c) A.W. Castleman, Jr., B.D. Kay, V. Hermann, P.M. Holland and T.D. Mark, Surf. Sci. 106, 179 (1981).

   d) K.L. Saenger, G.M. McClelland and D.R. Herschbach, J. Phys. Chem. 85, 3333 (1981).

   e) T.R. Hays, W. Henke, H.L. Selzle and E.W. Schlag, Chem. Phys. Lett. 77, 19 (1981).

3. a) F. Li, J. Lee and E.R. Bernstein, J. Phys. Chem. 87, 1175 (1983).

   b) J. Lee, F. Li and E.R. Bernstein, J. Phys. Chem. 87, 1180 (1983).

   c) F. Li, J. Lee and E.R. Bernstein, J. Phys. Chem., 87, 254 (1983).

   d) J. Lee, F. Li and E.R. Bernstein, J. Phys. Chem., 87, 260 (1983).

   e) F. Li, J. Lee and E.R. Bernstein, J. Phys. Chem. 86, 3606 (1982).

   f) M.W. Schauer, J. Lee and E.R. Bernstein, J. Chem. Phys. 76, 2773 (1982).

   g) E.R. Bernstein and J. Lee, J. Chem. Phys. 74, 3159 (1981).

4. D.E. Powers, J.B. Hopkins and R.E. Smalley, J. Chem. Phys. 72, 5721 (1980).

5. a) J. Tusa, M. Sulkes and S.A. Rice, J. Chem. Phys. 73, 5897 (1980).

   b) J. Tusa, M. Sulkes, S.A. Rice and C. Jouvet, J. Chem. Phys. 76, 3513 (1982).

6. C. Jouvet, M. Sulkes and S.A. Rice, Chem. Phys. Lett. 84, 241 (1981).

7. N. Mikami, A. Hiraya, I Fujiwara and M. Ito, Chem. Phys. Lett. 74, 531 (1980).

8. a) J.C.D. Brand, D.R. Williams and T.J. Cook, J. Molec. Spectros. 20, 359 (1966).

   b) M. Quack and M. Stockburger, J. Molec. Spectros. 43, 87 (1972).

9. a) D.A. Chernoff and S.A. Rice, J. Chem. Phys. 70, 2511 (1979).

   b) D.A. Chernoff and S.A. Rice, J. Chem. Phys. 70, 2521 (1979).

   c) R. Scheps, D. Florida and S.A. Rice, J. Chem. Phys. 61, 1730 (1974).

10. a) S.A. Rice, Adv. Chem. Phys. 47, Part 1, 117 (1981).

    b) M. Sukes, J. Tusa and S.A. Rice, J. Chem. Phys. 72, 5733 (1980).

11. a) R.E. Smalley, J. Phys. Chem. 86, 3504 (1982).

    b) C.S. Parmenter, J. Phys. Chem. 86, 1735 (1982).

    c) S. Mukamel and R.E. Smalley, J. Chem. Phys. 73, 4156 (1980).

    d) A. Amirav, U. Even and J. Jortner, J. Phys. Chem. 86, 3345 (1982).

    e) P.R. Stannard and W.M. Gelbart, J. Phys. Chem. 85, 3592 (1981).

    f) F.M. Behlen, N. Mikami and S.A. Rice, Chem. Phys. Lett. 60, 364 (1979).

12. a) D.H. Levy, Adv. Chem. Phys. 47, Part 1, 323 (1981).

    b) J.E. Kenny, K.E. Johnson, W. Sharfin and D.H. Levy, J. Chem. Phys. 72, 1109 (1980).

    c) M.F. Vernon, J.M. Lisy, H.S. Kwok, D.J. Krajnovich, A. Tramer, Y.R. Shen and Y.T. Lee, J. Phys. Chem. 85, 3327 (1981).

13. a) G.M. McClelland, K.L. Saenger, J.J. Valentini and D.R. Herschbach, J. Phys. Chem. 83, 947 (1979).

    b) G. Ewing, Chem. Phys. 29, 253 (1978).

    c) B. Blaney and G. Ewing, Ann. Rev. Phys. Chem. 27, 553 (1976).

14. S.A. Rice and C. Cerjan, to be published.

15. a) J.H. Brophy and C.T. Rettner, Chem. Phys. Lett. 67, 351 (1979).

b) T.G. Dietz, M.A. Duncan, M.G. Liverman and R.E. Smalley, Chem. Phys. Lett. 70, 246 (1980).

c) J.B. Hopkins, D.E. Powers and R.E. Smalley, J. Phys. Chem. 85, 3739 (1981).

d) D.M. Lubman, R. Naaman and R.N. Zare, J. Chem. Phys. 72, 3034 (1980).

16. a) R.E. Smalley, D.H. Levy and L. Wharton, J. Chem. Phys. 64, 3266 (1976).

b) D.H. Levy, L. Wharton and R.E. Smalley, Chemical and Biochemical Applications of Lasers, Vol II., pp. 1-41 (Academic Press, New York, 1977).

17. R.E. Smalley, L. Wharton, D.H. Levy and D.W. Chandler, J. Chem. Phys. 68, 2487 (1978).

18. K. Law, M.W. Schauer and E.R. Bernstein, unpublished results.

19. D.V. Brumbaugh, J.E. Kenny and D.H. Levy, J. Chem. Phys. 78, 3415 (1983).

TABLE I

Fluorescence excitation spectrum near 0_0^0 (34031 cm^{-1}) at 600 psi backing pressure (see Figure 2).

Peak	Position (Å)	Relative Position (cm^{-1})	Assignment
1	2938.5	0	Monomer
2	2937.8	7.9	vdW
3	2937.6	10.8	vdW
4	2937.0	17.7	vdW
5	2936.7	20.4	vdW
6	2936.2	26.4	vdW

TABLE II

a. Fluorescence excitation spectrum near $10b_0^2$ (34379 cm^{-1}) at 800 psi backing pressure (see Figure 4).

Peak	Position (Å)	Relative Position (cm^{-1})	Assignment
1	2908.7	0	$10b_0^2$ monomer
2	2908.3	5.9	$16a_0^2$ monomer
3	2907.6	13.1	vdW
4	2907.4	16.0	vdW
5	2907.0	20.5	vdW
6	2906.9	22.4	vdW
7	2906.3	29.1	monomer

b. Fluorescence excitation spectrum near $6a_0^1$ (34523 cm^{-1}) at 400 psi backing pressure (see Figure 4).

Peak	Position (Å)	Relative Position (cm^{-1})	Assignment
1	2896.6	0	$6a_0^1$ monomer
2	2896.0	7.5	vdW
3	2895.8	9.9	vdW
4	2895.2	16.8	vdW
5	2895.0	19.4	vdW
6	2894.6	24.2	monomer
7	2893.8	33.4	monomer

TABLE II (cont.)

c. Fluorescence excitation spectrum near I_0^2 (34790 cm^{-1}) at 900 psi backing pressure (see Figure 4).

Peak	Position (Å)	Relative Position (cm^{-1})	Assignment
1	2874.4	0	I_0^2 monomer
2	2873.7	8.0	vdW
3	2873.6	9.7	vdW
4	2872.9	17.6	monomer
5	2872.1	27.2	monomer

d. Fluorescence excitation spectrum near 1_0^1 (34829 cm^{-1}) at 800 psi backing pressure (see Figure 4).

Peak	Position (Å)	Relative Position (cm^{-1})	Assignment
1	2871.2	0	1_0^1 monomer
2	2870.8	4.4	vdW
3	2870.4	9.6	?
4	2869.8	17.0	vdW
5	2869.5	19.9	vdW
6	2869.1	25.1	vdW
7	2868.9	27.4	vdW

TABLE III

Dispersed emission spectrum pumping 0_0^0 (34031 cm^{-1}) at 200 psi backing pressure (see Figure 8).

Position (Å)	Relative Position (cm^{-1})	Relative Intensity	Assignment[a] 0_0^0
2975.7	425	100	I_2^0
2985.1	531	76	$6a_1^0$
3011.4	824	57	1_1^0 [b]
3023.0	951	83	$I_2^0 6a_1^0$
3026.8	993	19	?
3027.9	1005	37	12_1^0 [b]
3030.2	1030	29	$18a_1^0$
3033.0	1060	19	$6a_2^0$
3050.4	1248	68	$I_2^0 1_1^0$
3053.5	1282	24	$9a_1^0$
3060.0	1351	26	$6a_1^0 1_1^0$
3067.0	1426	36	$I_2^0 12_1^0$
3069.7	1455	29	$I_2^0 18a_1^0$
3072.0	1479	30	$I_2^0 6a_2^0$

(a) Families are assigned together in a column and labeled with the highest energy transition of the family.

(b) The assignment of 1 and 12 follow the convention of refs. 9 and 4.

TABLE IV

a. Unrelaxed emission from $10b_0^2$ (34379 cm^{-1}) at 100 psi backing pressure (see Figure 9).

Position (Å)	Relative Position (cm^{-1})	Assignment[a] $10b_2^2$
2945.9	433	$10b_2^2$
2982.8	853	$10b_2^2 I_2^0$
2992.8	965	$10b_2^2 6a_1^0$
3019.3	1259	$10b_2^2 1_1^0$
3030.8	1384	$10b_2^2 I_2^0 6a_1^0$
3035.6	1437	$10b_2^2 12_1^0$
3057.8	1676	$10b_2^2 I_2^0 1_1^0$

b. Unrelaxed emission from $16a_0^2$ (34385 cm^{-1}) at 70 psi backing pressure (see Figure 9).

Position (Å)	Relative Position (cm^{-1})	Assignment[a] $16a_2^2$
2978.1	807	$16a_2^2$
3016.4	1233	$16a_2^2 I_2^0$
3025.8	1336	$16a_2^2 6a_1^0$
3053.1	1631	$16a_2^2 1_1^0$
3064.9	1758	$16a_2^2 I_2^0 6a_1^0$
3093.4	2058	$16a_2^2 I_2^0 1_1^0$

TABLE IV (cont.)

c. Unrelaxed emission from I_1^1 (34326 cm^{-1}) at 150 psi backing pressure (see Figure 9).

Position (Å)	Relative Position (cm^{-1})	Assignment[a] I_1^1
2958.5	525	$I_1^1 6a_1^0$
2970.1	657	I_3^1
2984.7	822	$I_1^1 1_1^0$
3000.4	997	$I_1^1 12_1^0$
3003.5	1031	$I_1^1 18a_1^0$
3005.7	1056	$I_1^1 6a_2^0$

(a) Families are assigned together in a column and labeled with the highest energy transition of the family.

TABLE V

Dispersed emission spectra pumping $10b_0^2$ monomer (34379 cm^{-1}) at 600 psi backing pressure and a van der Waals peak (34392 cm^{-1}) [peak 3, Table II] at 600 psi backing pressure (see Figure 10).

Position (Å)	Relative Position (cm^{-1})	Monomer Relative Intensity	vdW Relative Intensity	Assignment[a] $10b_2^2$	$10b_1^1$	0_0^0	$16a_2^2$	$16a_1^1$
2938.6	349	12	4			0_0^0		
2942.2	391	41	49		$10b_1^1$			
2945.9	433	100		$10b_2^2$				
2959.6	591		100					$16a_1^1$
2975.6	772	15	4			I_2^0		
2979.0	811	37	46		$10b_1^1I_2^0$		$16a_2^2$	
2982.8	853	99		$10b_2^2I_2^0$				
2985.1	879	7	3			$6a_1^0$		
2988.8	921	15	24		$10b_1^16a_1^0$			
2992.7	965	49		$10b_2^26a_1^0$				
2997.1	1014		95					$16a_1^1I_2^0$
3006.8	1121		46					$16a_1^16a_1^0$
3011.3	1171	9				1_1^0		
3015.3	1215	15	20		$10b_1^11_1^0$			
3016.9	1233	21					$16a_2^2I_2^0$	
3019.3	1259	49		$10b_2^21_1^0$				

TABLE V (cont.)

Position (Å)	Relative Position (cm^{-1})	Monomer Relative Intensity	vdW Relative Intensity	Assignment[a] $10b_2^2$	$10b_1^1$	0_0^0	$16a_2^2$	$16a_1^1$
3023.1	1300	15	4			$I_2^0 6a_1^0$		
3026.8	1341	30	31		$10b_1^1 I_2^0 6a_1^0$			
3030.8	1384	59		$10b_2^2 I_2^0 6a_1^0$				
3034.2	1421		49					$16a_1^1 1_1^0$

(a) Families are assigned together in a column and labeled with the highest energy transition of the family.

TABLE VI

Dispersed emission spectra pumping $6a_0^1$ monomer (34523 cm^{-1}) and a van der Waals peak [peak 2, Table II] (see Figure 11).

Position (Å)	Relative Position (cm^{-1})	Relative Intensity (Monomer 200 psi)	Relative Intensity (vdW Peak 600 psi)	Assignment[a]			
				$6a_0^1$	I_1^1	0_0^0	$16a_1^1$
2913.6	201	6	68		I_1^1		
2932.7	425	42	20	$6a_0^1I_2^0$			
2938.8	496	2	45			0_0^0	
2941.9	531	21	64	$6a_1^1$			
2959.2	730	3	77		$I_1^16a_1^0$		$16a_1^1$
2967.3	823	27	73	$6a_0^1I_1^0$			
2970.7	861	3	21		I_3^1		
2975.5	915	3	73			I_2^0	
2978.5	949	32	64	$6a_1^1I_2^0$			
2983.5	1005	24		$6a_0^112_1^0$			
2985.3	1025	17	100	$6a_0^118a_1^0$	$I_1^1I_1^0$	$6a_1^0$	
2988.3	1059	80	54	$6a_2^1$			
2996.3	1157	3	66				$16a_1^1I_2^0$
3001.4	1205	3	52		$I_1^112_1^0$		
3005.5	1251	32	36	$6a_0^1I_2^0I_1^0$			$16a_1^16a_1^0$

TABLE VI (cont.)

Position (Å)	Relative Position (cm^{-1})	Relative Intensity (Monomer 200 psi)	Relative Intensity (vdW Peak 600 psi)	Assignment[a] $6a_0^1$	I_1^1	0_0^0	$16a_1^1$
3008.3	1282	18		$6a_0^1 9a_1^0$			
3011.8	1320	3	50			1_1^0	
3014.9	1355	18	18	$6a_1^1 1_1^0$			
3017.3	1381	3	29		$I_3^1 6a_1^0$		
3021.1	1423	20	45	$6a_0^1 I_2^0 12_1^0$			
3026.1	1477	100	79	$6a_2^1 I_2^0$	$I_1^1 9a_1^0$	$I_2^0 6a_1^0$	

(a) Families are assigned together in a column and labeled with the highest energy transition of the family.

TABLE VI

Dispersed emission spectrum of I_0^2 (34790 cm^{-1}) at 300 psi backing pressure (see Figure 12).

Position (Å)	Relative Position (cm^{-1})	Relative Intensity	Assignment[a]				
			I_0^2	I_1^1	$I_1^1 16a_1^1$	$10b_2^2$	0_0^0
2909.7	422	100	I_2^2				
2913.4	466	10		I_1^1			
2918.8	530	40	$I_0^2 6a_1^0$				
2920.1	545	40					
2935.9	729	6			$I_1^1 16a_1^1$		(0_0^0)
2943.8	820	46	$I_0^2 1_1^0$			$(10b_2^2)$	
2955.0	949	72	$I_2^2 6a_1^0$				
2958.7	992	36	$I_0^2 12_1^0$	$I_1^1 6a_1^0$			
2961.9	1028	15	$I_0^2 18a_1^0$				
2964.5	1058	45	$I_0^2 6a_2^0$				
2965.9	1073	20					
2966.9	1085	47	I_4^2				
2975.9	1187	14					I_2^0
2977.4	1204	14					
2981.1	1245	17	$I_2^2 1_1^0$		$I_1^1 16a_1^1 6a_1^0$		
2981.7	1252	16				$10b_2^2 I_2^0$	

TABLE VII (cont.)

Position (Å)	Relative Position (cm^{-1})	Relative Intensity	Assignment[a]				
			I_0^2	I_1^1	$I_1^1 16a_1^1$	$10b_2^2$	0_0^0
2984.4	1283	22	$I_0^2 9a_1^0$	$I_1^1 1_1^0$			
2990.4	1350	36	$I_0^2 6a_1^0 1_1^0$				
2991.7	1364	15				$10b_2^2 6a_1^0$	
2992.3	1371	15					
2997.3	1427	34	$I_2^2 12_1^0$				

(a) Families are assigned together in a column and labeled with the highest energy transition of the family.

TABLE VIII

Dispersed emission spectrum of 1_0^1 (34892 cm^{-1}) at 600 psi backing pressure (see Figure 13).

Position (Å)	Relative Position (cm^{-1})	Assignment[a]		
		1_0^1	I_1^1	$10b_2^2 16a_1^1$
2906.6	425	$1_0^1 I_2^0$		
2913.7	509		I_1^1	
2915.6	531	$1_0^1 6a_1^0$		
2938.3	796			
2940.7	824	1_1^1		
2951.8	951	$I_0^1 I_2^0 6a_1^0$		
2956.5	1005	$1_0^1 12_1^0$		
2958.7	1030	$1_0^1 18a_1^0$		
2959.5	1040		$I_1^1 6a_1^0$	
2961.3	1060	$1_0^1 6a_2^0$		
2966.6	1120			$10b_2^2 16a_1^1$
2970.9	1169		I_3^1	
2975.5	1221			
2977.9	1248	$1_1^1 I_2^0$		
2980.9	1282	$1_0^1 9a_1^0$		
2985.2	1330		$I_1^1 1_1^0$	
2987.0	1351	$1_1^1 6a_1^0$		
2993.7	1426	$1_0^1 I_2^0 12_1^0$		
2996.3	1455	$1_0^1 I_2^0 18a_1^0$		
2998.5	1479	$1_0^1 I_2^0 6a_2^0$		
3001.7	1514		$I_1^1 12_1^0$	
3004.2	1542		$I_1^1 18a_1^0$	$10b_2^2 16a_1^1 I_2^0$
3006.2	1564	$1_0^1 18a_1^0 6a_1^0$	$I_1^1 6a_2^0$	
3011.2	1620			

TABLE VIII (cont.)

Position (Å)	Relative Position (cm^{-1})	Assignment[(a)]		
		1_0^1	I_1^1	$10b_2^2 16a_1^1$
3013.9	1649	1_2^1		$10b_2^2 16a_1^1 6a_1^0$
3019.1	1706	$1_0^1 9a_1^0 I_2^0$	$I_3^1 6a_1^0$	
3022.8	1747			
3026.3	1785	$1_1^1 6a_1^0 I_2^0$	$I_1^1 9a_1^0$	
3027.7	1801			
3028.8	1813	$1_0^1 6a_1^0 9a_1^0$		
3030.1	1827			
3032.7	1855	$1_1^1 18a_1^0$		
3033.5	1864		$I_1^1 1_1^0 6a_1^0$	
3040.9	1944			$10b_2^2 16a_1^1 1_1^0$
3045.0	1988	$1_0^1 18a_1^0 6a_1^0 I_2^0$	$I_3^1 1_1^0$	
3049.6	2035	$1_0^1 18a_1^0 12_1^0$		
3050.3	2045		$I_1^1 6a_1^0 12_1^0$	
3052.1	2065	$1_0^1 18a_2^0 (1_2^1 I_2^0)$		

(a) Families are assigned together in a column and labeled with the highest energy transition of the family.

FIGURE CAPTIONS

FIGURE 1: Supersonic Molecular Jet Apparatus

I	-	Chamber I containing FE and DE experiments
II	-	Chamber II containing TOFMS experiment
TS	-	Translation stage for positioning the nozzle
OVBP	-	Oil vapor booster pump backed by a mechanical pump
G1	-	Cold cathode gauge attached by compression fitting
N	-	Continuous nozzle
M	-	Spherical reflector
L1	-	100mm plano - convex lens
L2	-	300mm plano - convex lens
A	-	Aperture
L3	-	Lens
PMT	-	Photomultiplier tube
S	-	Skimmer
GV1	-	2" gate valve
GV2	-	10" gate valve
WB	-	Water baffle
DP	-	10" diffusion pump
IR	-	Ionization region of the mass spectrometer
FT	-	Flight tube of the mass spectrometer
D	-	Multichannel plate detector
T	-	Liquid nitrogen trap
G2	-	Ionization gauge
W	-	Alignment window

FIGURE 2

FE spectra of the 0_0^0 region of aniline expanded with helium at various backing pressures. The monomer peak is at 34031 cm^{-1} (see Table I). The decrease in aniline monomer intensity is largely due to the decrease in concentration of aniline as the backing pressure is increased. These spectra show how the van der Waals absorption peaks grow in with increasing backing pressure.

FIGURE 3

Plots of the natural log of the intensity of various peaks near the 0_0^0 feature realtive to the intensity of the monomer vs. the natural log of the backing pressure. The curves are labeled with the peak numbers found in Table I. All the curves have already begun to deviate from linearity at the lowest pressures.

FIGURE 4

FE spectra in the region of various vibronic transitions of aniline. The monomer peaks are aligned and an approximate relative energy scale is given at the bottom (see Table II). No correction has been made for difference in dispersion between the spectra. All show similar patterns of van der Waals peaks to higher energy.

FIGURE 5

TOF mass spectra taken at various backing pressures while pumping the monomer 0_0^0 absorption feature. The main peak is the aniline monomer peak at 93 AMU. One C^{13} peak is visible to the right of the monomer and peaks associated with $AnHe_1$, $AnHe_2$ and $AnHe_3$ grow in as the backing pressure is increased. This clearly indicates that as An is pumped $AnHe_x$ clusters are also pumped.

FIGURE 6

TOF mass spectra obtained by pumping various van der Waals peaks near 0_0^0. The peaks being pumped are labeled by the numbers from Table I. Preliminary assignments of the absorption bands being pumped can be made from these spectra (see text).

FIGURE 7

TOF mass spectra obtained by pumping various features near $10b_0^2$ at 900 psi. The peaks being pumped are labeled by the numbers given in Figure 4, top spectrum. It is clear from these spectra that the van der Waals species dissociate before being detected and that recombination does not occur in any of these experiments.

FIGURE 8

DE spectrum obtained by pumping the 0_0^0 monomer feature and part of the DE spectrum obtained by pumping the van der Waals peak labeled 3 in Figure 2. The calculated peak positions of the 0_0^0 family are indicated below the monomer spectrum. Emission from the van der Waals feature is essentially identical to emission from the monomer feature (see Table III).

FIGURE 9

DE spectra obtained by pumping I_1^1, $16a_0^2$ and $10b_0^2$ monomer vibronic transitions at low backing pressures. The calculated positions of unrelaxed family members are indicated below each spectrum. These spectra show minimal relaxation and clearly show fluorescence from three different vibronic levels in the excited state (see Table IV).

FIGURE 10

DE spectra obtained by pumping the $10b_0^2$ monomer peak and the van der Waals peak labeled 3 in the top spectrum of Figure 4. This peak is undoubtedly a composite of a $10b^2$ and $16a^2$ van der Waals molecule related feature, thus explaining the large $16a_1^1$ intensity. Emission from the van der Waals peak is totally relaxed (see Table V). The calculated positions of various families 4are indicated below each spectrum.

FIGURE 11

DF spectra obtained by pumping the $6a_0^1$ monomer peak at low and high pressures, and the van der Waals peak labeled 3 in the second spectrum of Figure 4. These spectra show more relaxation for higher backing pressure and for pumping van der Waals peaks (see Table VI). The calculated positions of various families are indicated below the high pressure monomer spectrum.

FIGURE 12

DF spectrum obtained by pumping the 1_0^2 monomer absorption peak. Even at moderate pressures this spectrum shows relaxation to a large number of vibronic levels (see Table VII). Most of this relaxed emission is attributed to vibrational predissociation of van der Waals complexes (see text). The calculated positions of several relaxation families are given below the spectrum.

FIGURE 13

DF spectra obtained by pumping the 1_0^1 monomer absorption band at two backing pressures. Several relaxation families grow in at high pressure (see Table VIII) again indicating that the relaxation is due to vibrational predissociation of van der Waals clusters. Their calculated positions are indicated below the high pressure spectrum.

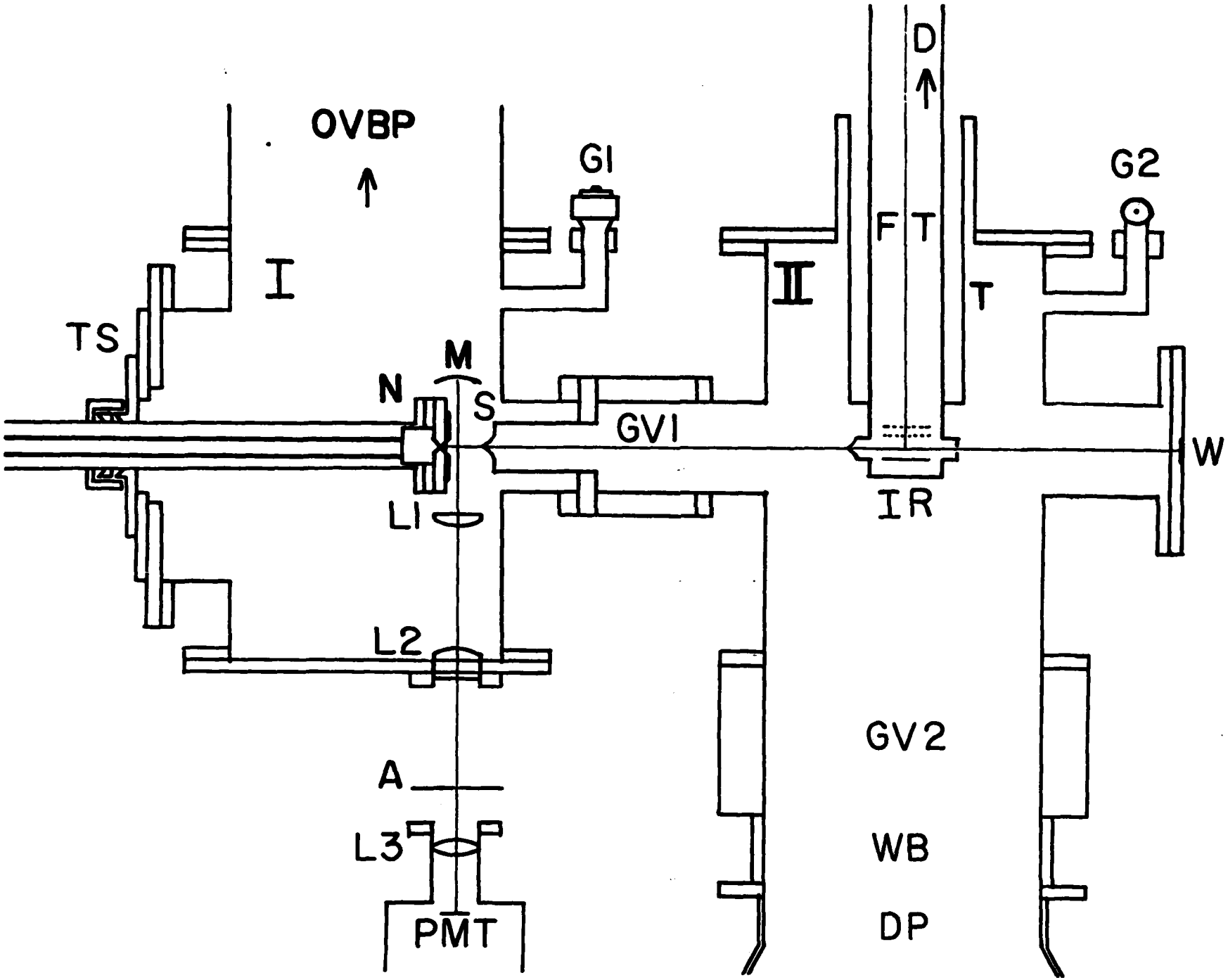
D
OVBP
G1
G2
F
T
I
II
T
TS
M
N
S
GV1
W
IR
L1
L2
GV2
A
L3
WB
PMT
DP

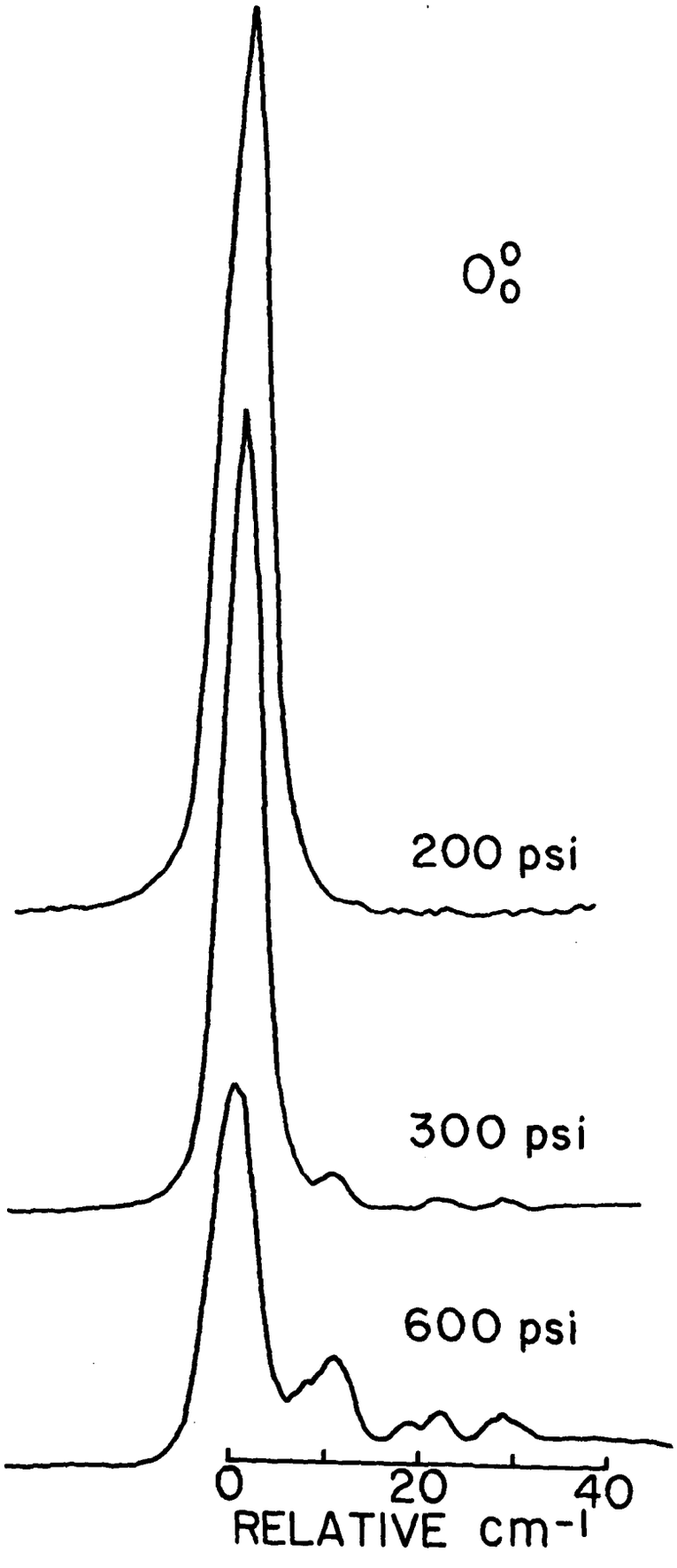
0°
200 psi
300 psi
600 psi
0
20
40
RELATIVE cm-1

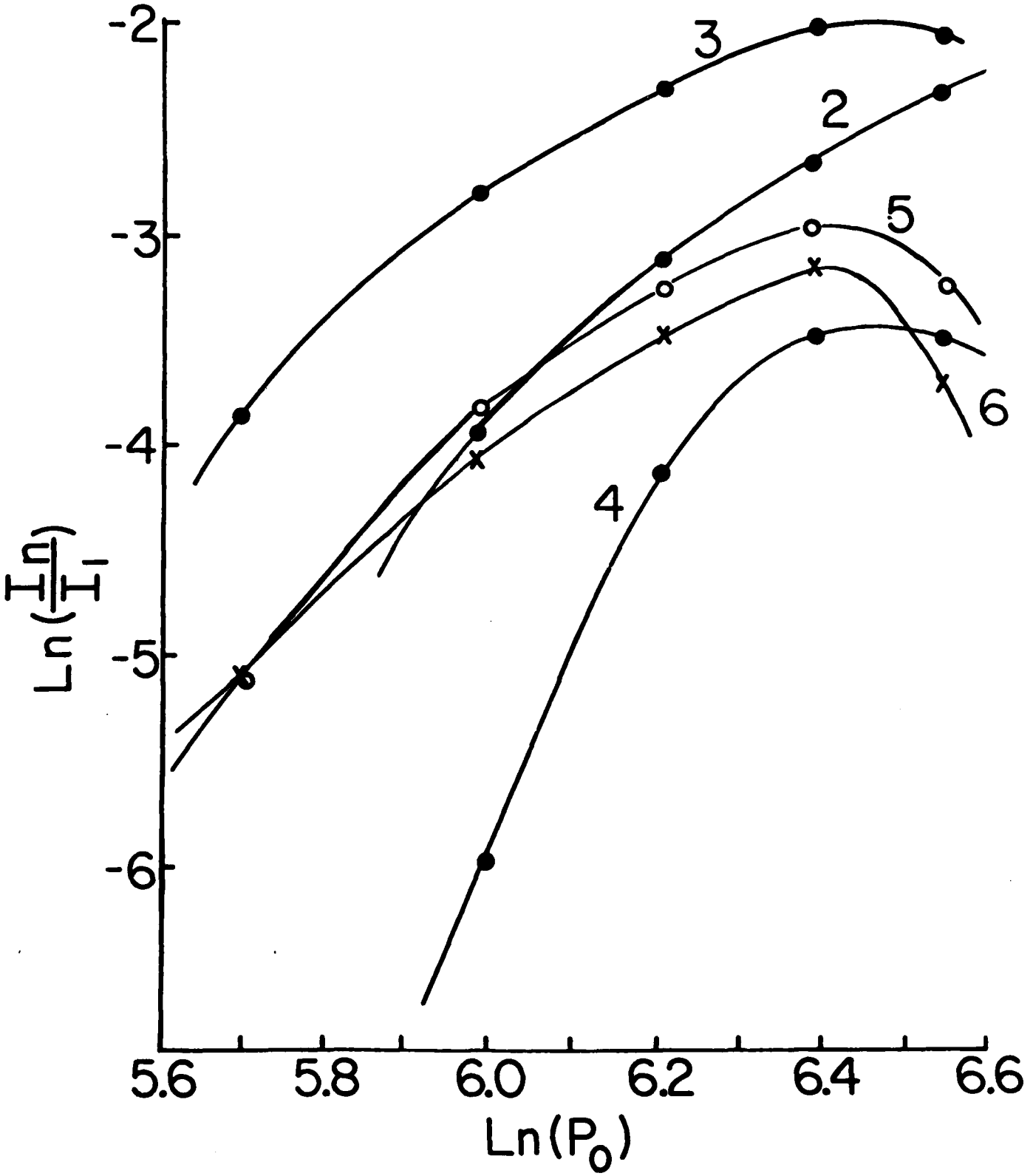
-2
-3
-4
-5
-6
3
2
5
6
4
$Ln(\frac{H_n}{H_1})$
5.6
5.8
6.0
6.2
6.4
6.6
$Ln(P_0)$

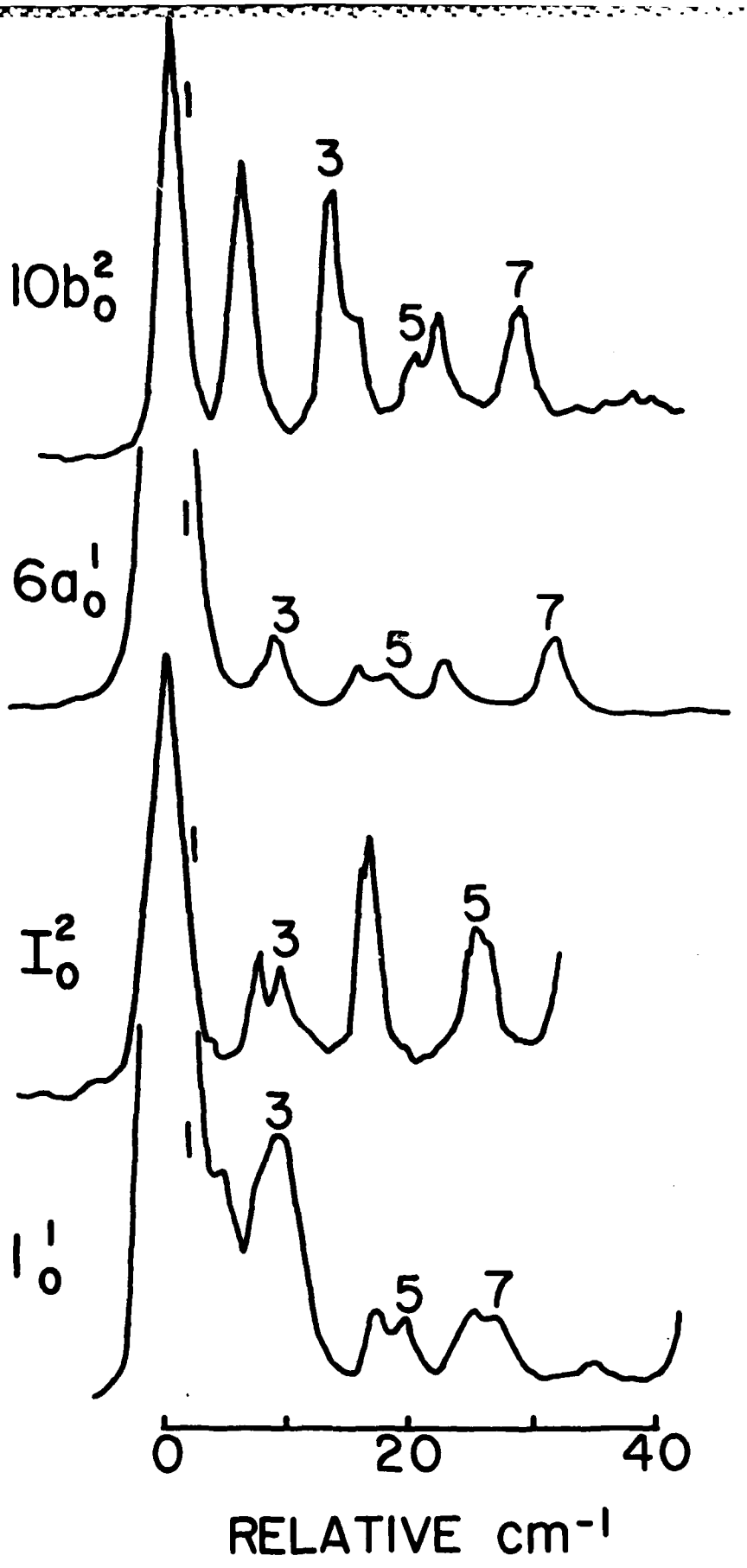
$10b_0^2$
$6a_0^1$
I_0^2
1_0^1
1
3
5
7
0
20
40
RELATIVE cm^{-1}

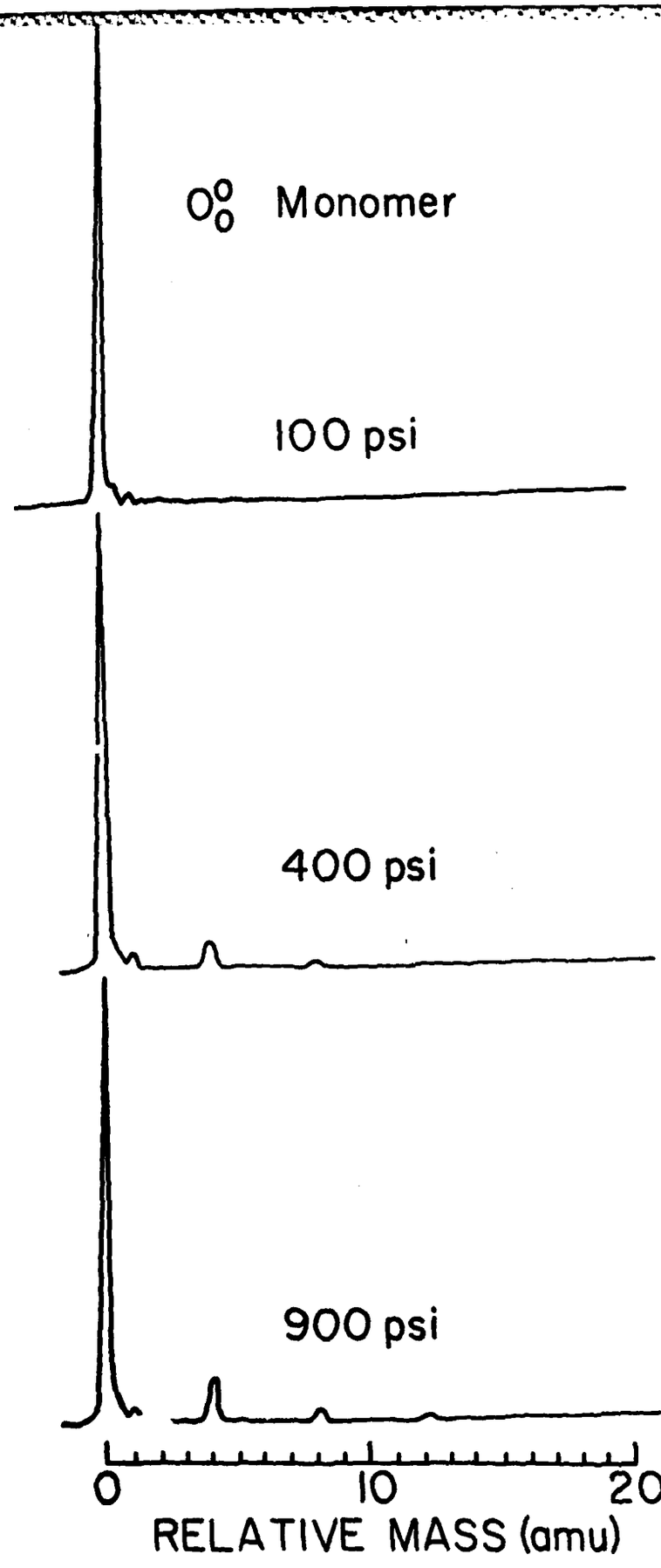
O_2^0 Monomer
100 psi
400 psi
900 psi
0
10
20
RELATIVE MASS (amu)

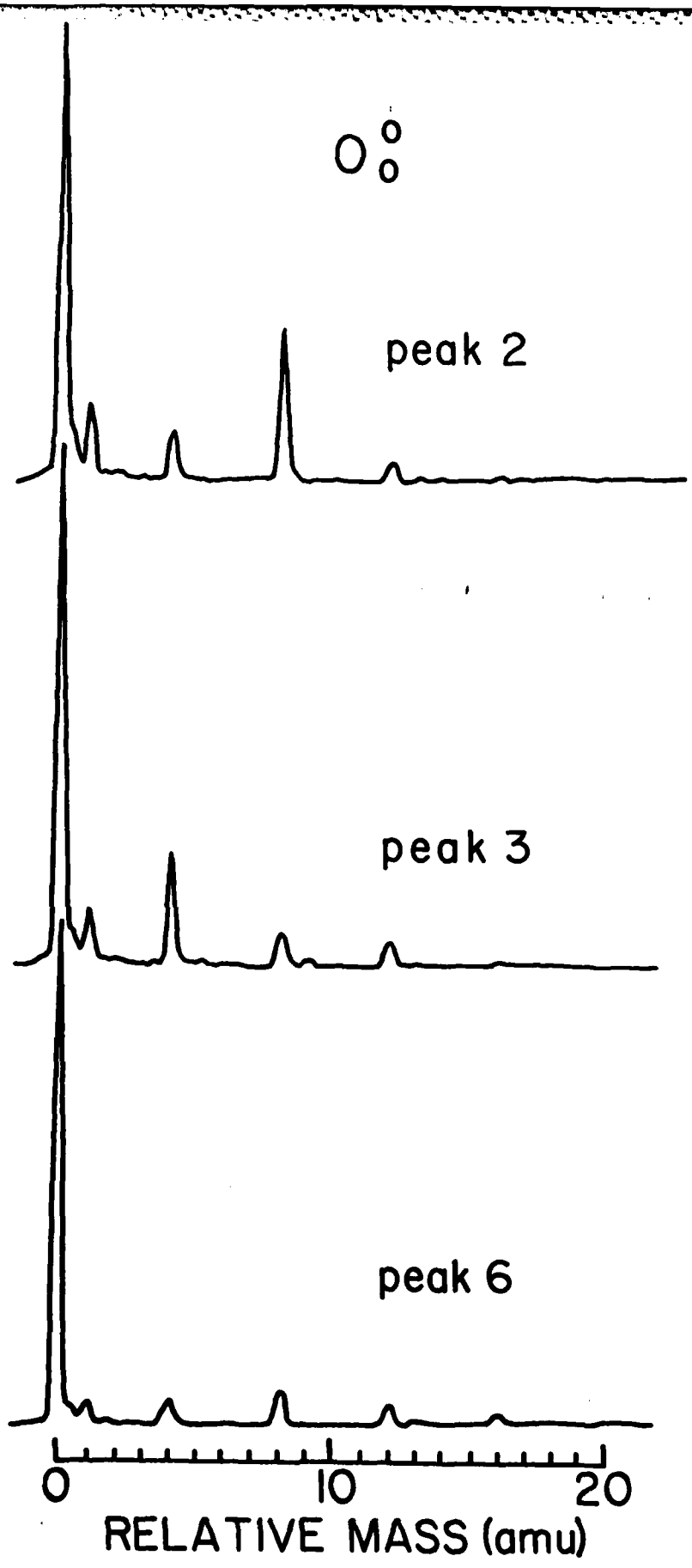
O O
peak 2
peak 3
peak 6
0
10
20
RELATIVE MASS (amu)

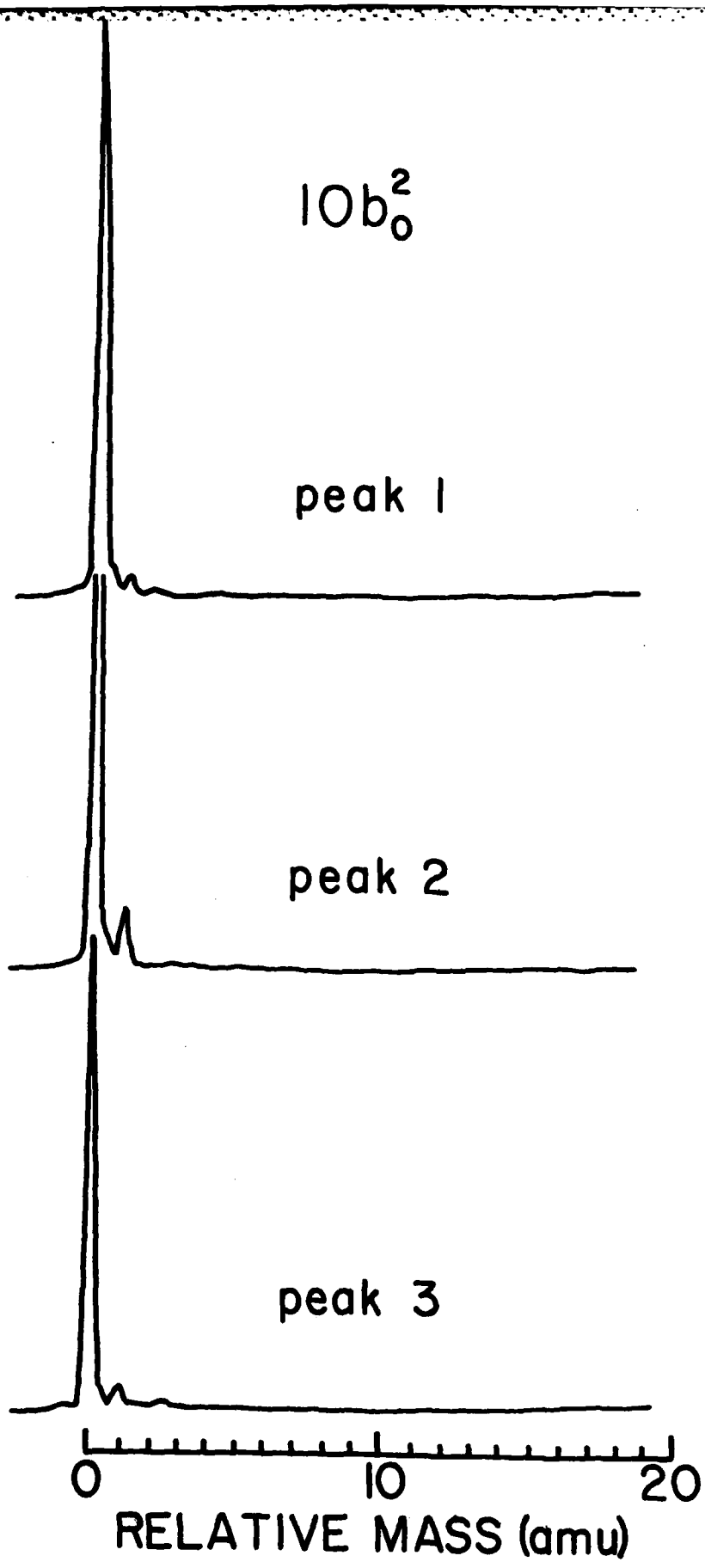
$10b_0^2$
peak 1
peak 2
peak 3
0
10
20
RELATIVE MASS (amu)

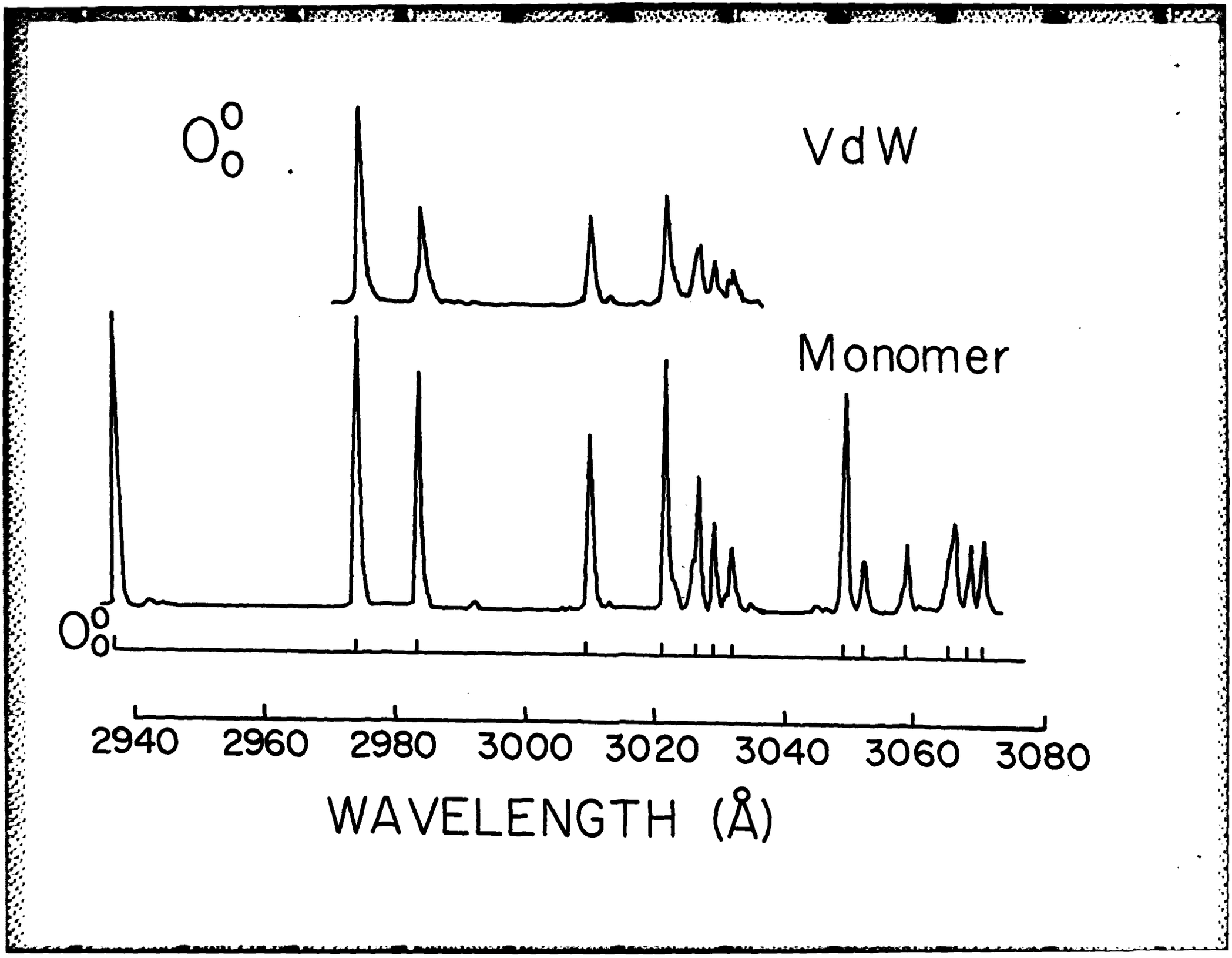
VdW
Monomer
2940
2960
2980
3000
3020
3040
3060
3080
WAVELENGTH (Å)

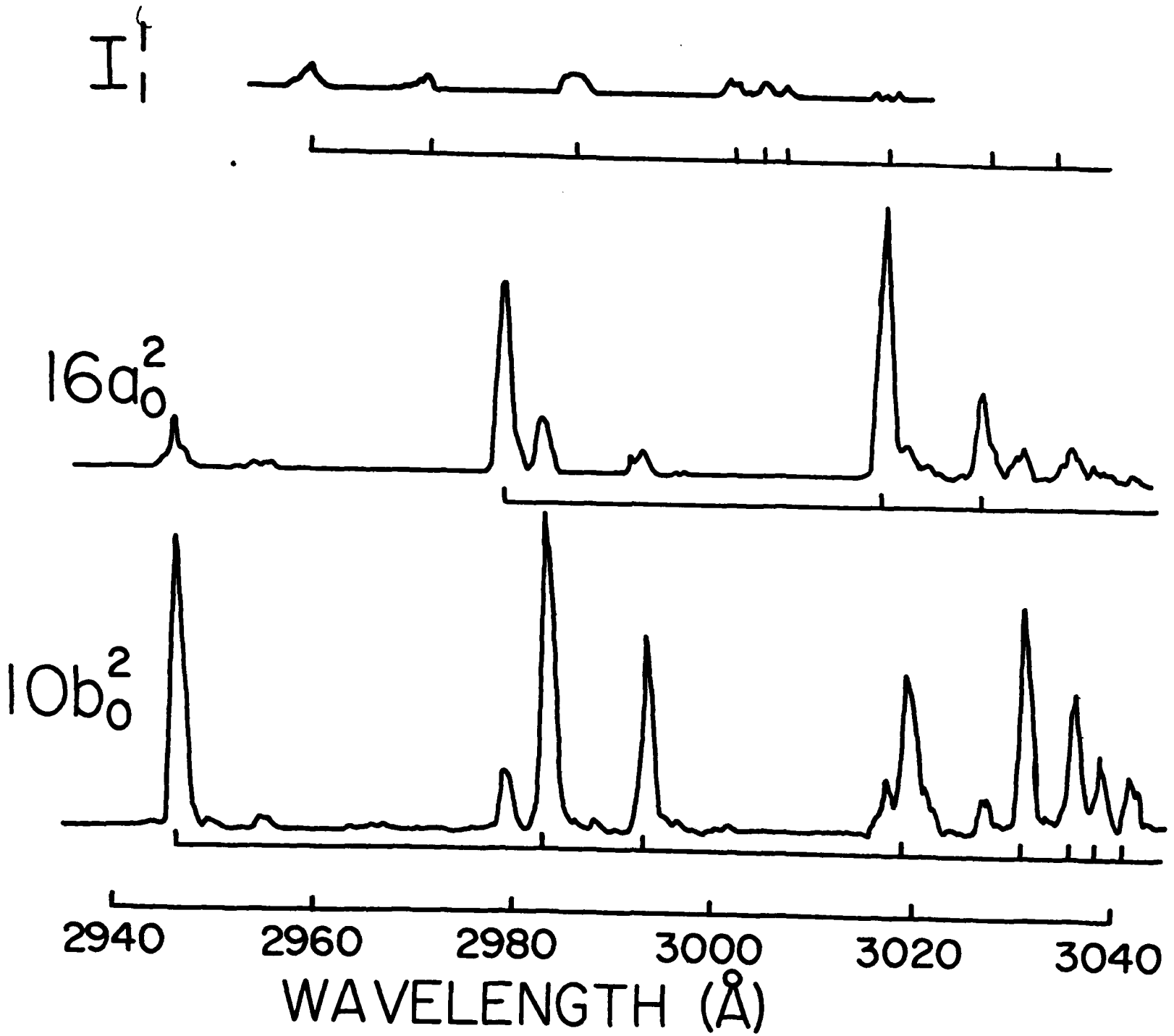
I_1^1
$16a_0^2$
$10b_0^2$
2940
2960
2980
3000
3020
3040
WAVELENGTH (Å)

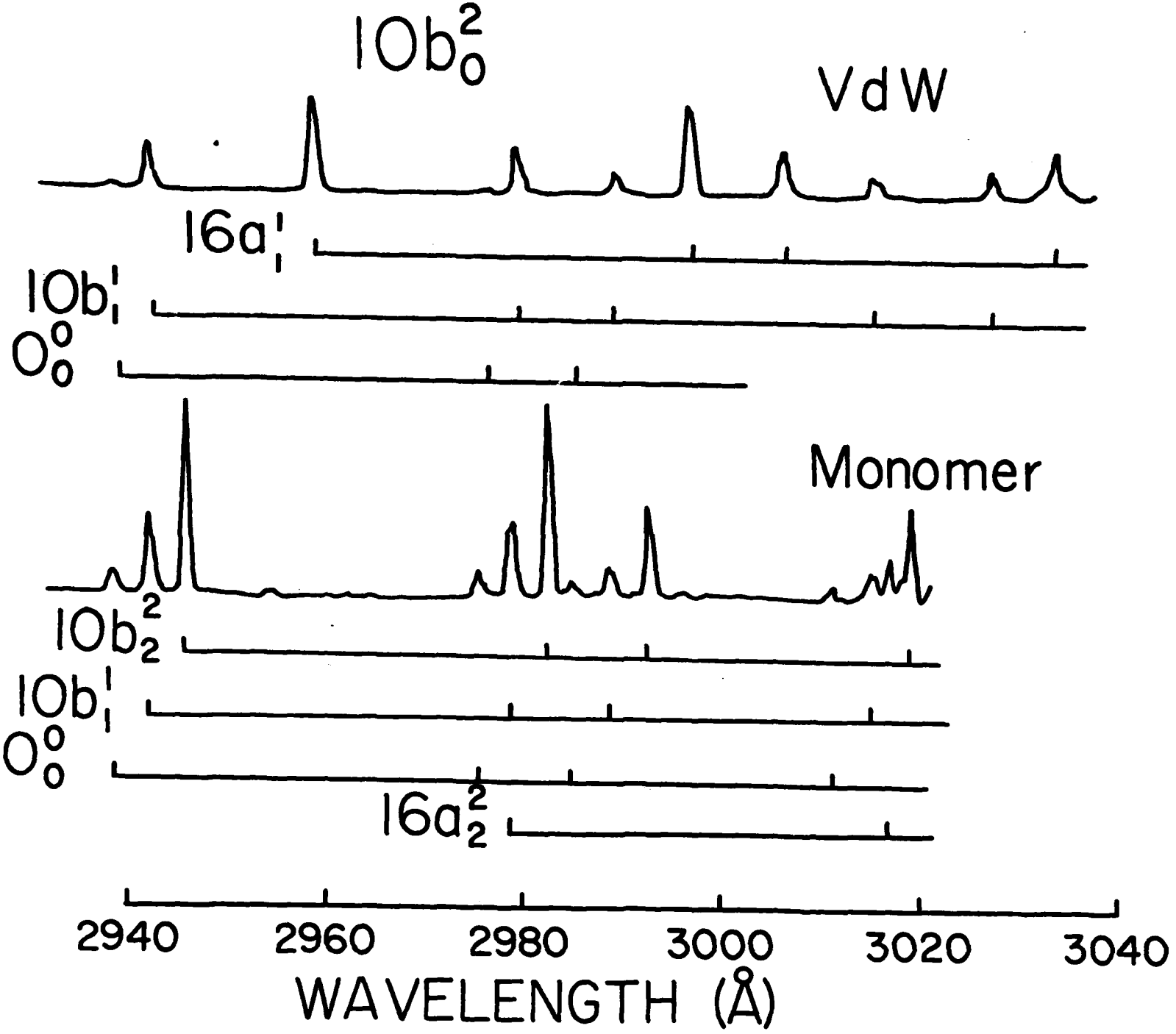
$10b_0^2$
VdW
$16a_1^1$
$10b_1^1$
0_0^0
Monomer
$10b_2^2$
$10b_1^1$
0_0^0
$16a_2^2$
2940
2960
2980
3000
3020
3040
WAVELENGTH (Å)

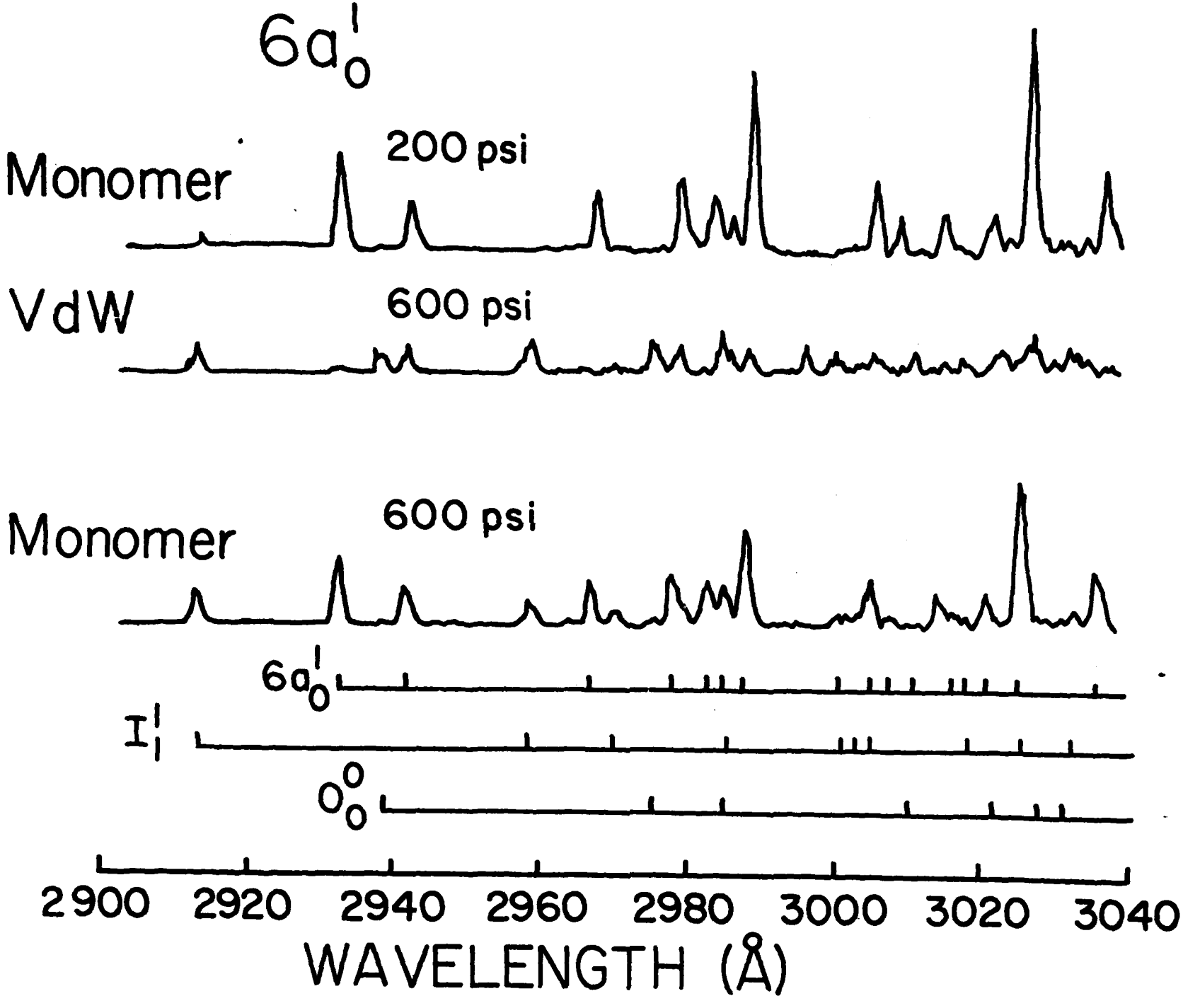
$6a_0^1$
Monomer
200 psi
VdW
600 psi
Monomer
600 psi
$6a_0^1$
I_1^1
0_0^0
2900 2920 2940 2960 2980 3000 3020 3040
WAVELENGTH (Å)

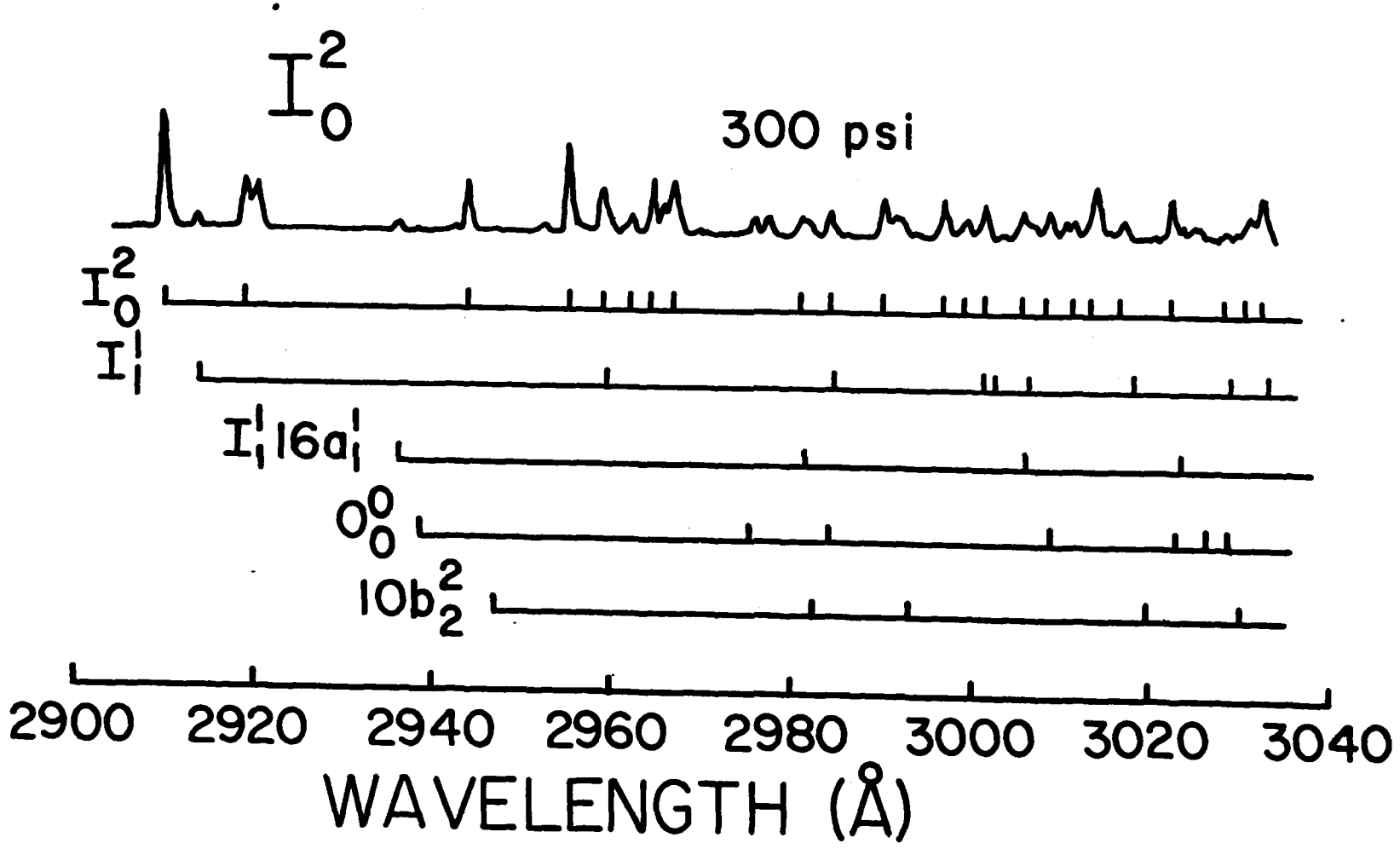
I_0^2
300 psi
I_0^2
I_1^1
$I_1^1 16a_1^1$
0_0^0
$10b_2^2$
2900
2920
2940
2960
2980
3000
3020
3040
WAVELENGTH (Å)

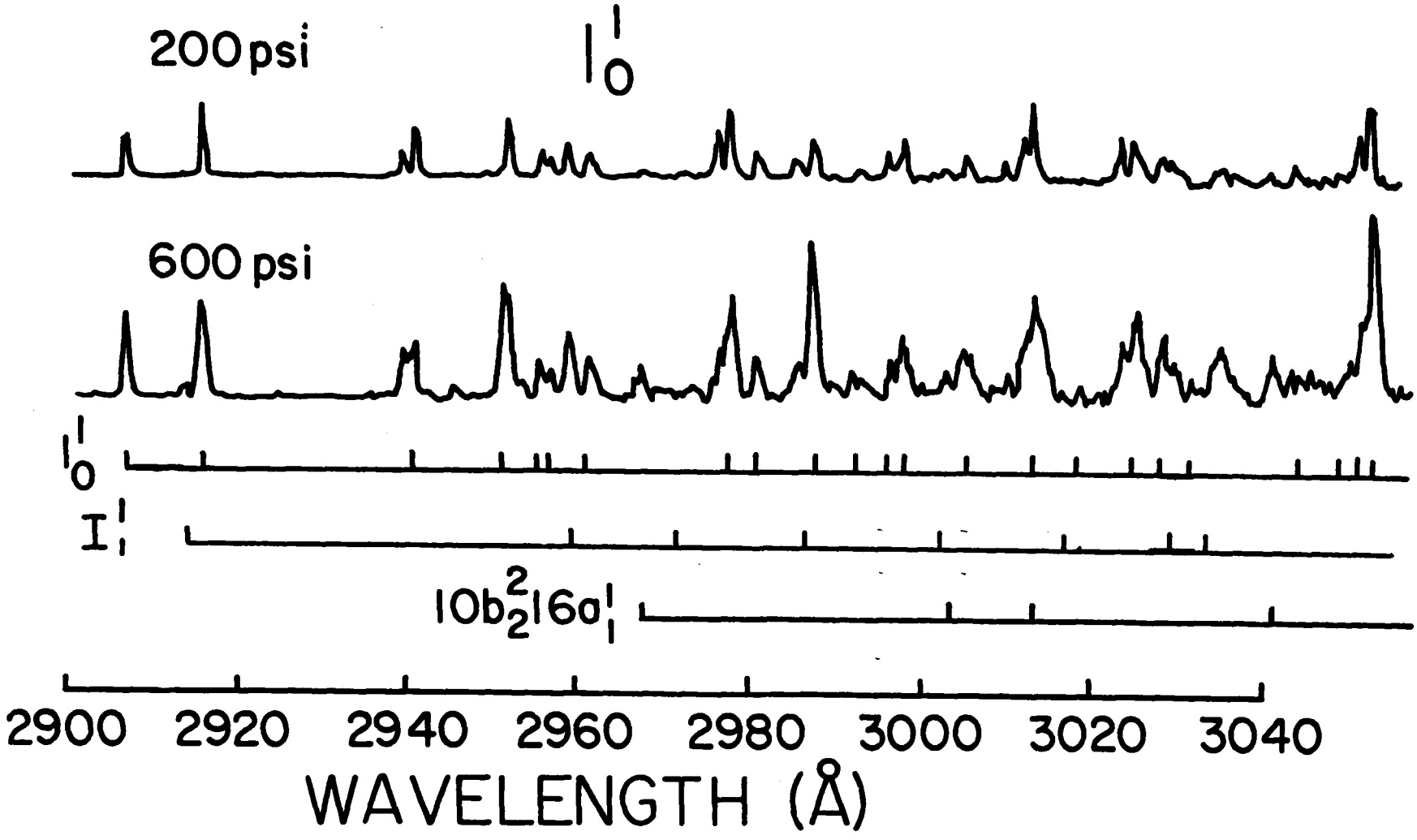
200 psi
1_0^1
600 psi
1_0^1
I_1^1
$10b_2^2 16a_1^1$
2900 2920 2940 2960 2980 3000 3020 3040
WAVELENGTH (Å)

TECHNICAL REPORT DISTRIBUTION LIST, GEN

	No. Copies
Office of Naval Research Attn: Code 472 800 North Quincy Street Arlington, Virginia 22217	2
ONR Western Regional Office Attn: Dr. R. J. Marcus 1030 East Green Street Pasadena, California 91106	1
ONR Eastern Regional Office Attn: Dr. L. H. Peebles Building 114, Section D 666 Summer Street Boston, Massachusetts 02210	1
Director, Naval Research Laboratory Attn: Code 6100 Washington, D.C. 20390	1
The Assistant Secretary of the Navy (RE&S) Department of the Navy Room 4E736, Pentagon Washington, D.C. 20350	1
Commander, Naval Air Systems Command Attn: Code 310C (H. Rosenwasser) Department of the Navy Washington, D.C. 20360	1
Defense Technical Information Center Building 5, Cameron Station Alexandria, Virginia 22314	12
Dr. Fred Saalfeld Chemistry Division, Code 6100 Naval Research Laboratory Washington, D.C. 20375	1
U.S. Army Research Office Attn: CRD-AA-IP P.O. Box 1211 Research Triangle Park, N.C. 27709	1
Naval Ocean Systems Center Attn: Mr. Joe McCartney San Diego, California 92152	1
Naval Weapons Center Attn: Dr. A. B. Amster, Chemistry Division China Lake, California 93555	1
Naval Civil Engineering Laboratory Attn: Dr. R. W. Drisko Port Hueneme, California 93401	1
Department of Physics & Chemistry Naval Postgraduate School Monterey, California 93940	1
Scientific Advisor Commandant of the Marine Corps (Code RD-1) Washington, D.C. 20380	1
Naval Ship Research and Development Center Attn: Dr. G. Bosmajian, Applied Chemistry Division Annapolis, Maryland 21401	1
Naval Ocean Systems Center Attn: Dr. S. Yamamoto, Marine Sciences Division San Diego, California 91232	1
Mr. John Boyle Materials Branch Naval Ship Engineering Center Philadelphia, Pennsylvania 19112	1

472:GAN:716:enj
78u472-608

TECHNICAL REPORT DISTRIBUTION LIST, GEN

	No. Copies
Mr. James Kelley DTNSRDC Code 2803 Annapolis, Maryland 21402	1
Mr. A. M. Anzalone Administrative Librarian PLASTEC/ARRADCOM Bldg 3401 Dover, New Jersey 07801	1

TECHNICAL REPORT DISTRIBUTION LIST, 051A

	No. Copies
Dr. M. A. El-Sayed Department of Chemistry University of California, Los Angeles Los Angeles. California 90024	1
Dr. C. A. Heller Naval Weapons Center Code 6059 China Lake, California 93555	1
Dr. J. R. MacDonald Chemistry Division Naval Research Laboratory Code 6110 Washington, D.C. 20375	1
Dr. G. B. Schuster Chemistry Department University of Illinois Urbana, Illinois 61801	1
Dr. A. Adamson Department of Chemistry University of Southern California Los Angeles, California 90007	1
Dr. M. S. Wrighton Department of Chemistry Massachusetts Institute of Technology Cambridge, Massachusetts 02139	1
Dr. M. Rauhut Chemical Research Division American Cyanamid Company Bound Brook, New Jersey 08805	1
Dr. J. I. Zink Department of Chemistry University of California, Los Angeles Los Angeles, California 90024	1
Dr. D. Haarer IBM San Jose Research Center 5600 Cottle Road San Jose, California 95143	1
Dr. John Cooper Code 6130 Naval Research Laboratory Washington, D.C. 20375	1
Dr. William M. Jackson Department of Chemistry Howard University Washington, DC 20059	1
Dr. George E. Walraffen Department of Chemistry Howard University Washington, DC 20059	1

END

FILMED

10-83

DTIC